MicroRNAs and Their Targets Are Differentially Regulated in Adult and Neonatal Mouse CD8+ T Cells

Erin M. Wissink,*[,1] Norah L. Smith,[†,1] Roman Spektor,[‡] Brian D. Rudd,[†,2] and Andrew Grimson[§,2]
*Graduate Field of Biochemistry, Molecular, and Cell Biology, [†]Department of Microbiology and Immunology, [‡]Graduate Field of Genetics, Genomics, and Development, and [§]Department of Molecular Biology and Genetics, Cornell University, Ithaca, New York 14853

ABSTRACT Immunological memory, which protects organisms from re-infection, is a hallmark of the mammalian adaptive immune system and the underlying principle of vaccination. In early life, however, mice and other mammals are deficient at generating memory CD8+ T cells, which protect organisms from intracellular pathogens. The molecular basis that differentiates adult and neonatal CD8+ T cells is unknown. MicroRNAs (miRNAs) are both developmentally regulated and required for normal adult CD8+ T cell functions. We used next-generation sequencing to identify mouse miRNAs that are differentially regulated in adult and neonatal CD8+ T cells, which may contribute to the impaired development of neonatal memory cells. The miRNA profiles of adult and neonatal cells were surprisingly similar during infection; however, we observed large differences prior to infection. In particular, miR-29 and miR-130 have significant differential expression between adult and neonatal cells before infection. Importantly, using RNA-Seq, we detected reciprocal changes in expression of messenger RNA targets for both miR-29 and miR-130. Moreover, targets that we validated include *Eomes* and *Tbx21*, key genes that regulate the formation of memory CD8+ T cells. Notably, age-dependent changes in miR-29 and miR-130 are conserved in human CD8+ T cells, further suggesting that these developmental differences are biologically relevant. Together, these results demonstrate that miR-29 and miR-130 are likely important regulators of memory CD8+ T cell formation and suggest that neonatal cells are committed to a short-lived effector cell fate prior to infection.

KEYWORDS microRNA regulation; adaptive immunity; development

THE majority of mammalian messenger RNAs (mRNAs) contain conserved target sites that bind microRNAs (miRNAs) (Friedman *et al.* 2009). Such target sites are typically located within the 3′ untranslated regions (3′ UTRs) of mRNAs, and binding of a miRNA to a target site predominantly causes the target's accelerated decay and resulting protein repression (Bartel 2009; Fabian *et al.* 2010; Guo *et al.* 2010; Eichhorn *et al.* 2014). Because mammals have hundreds of miRNAs, each of which can have hundreds of targets, most regulatory pathways incorporate miRNAs (Kim and Nam 2006). One prominent example of miRNAs impacting cellular processes is found in the immune system, where it is clear that different immune cells require specific miRNAs to develop and function (Xiao and Rajewsky 2009; Dooley *et al.* 2013; Kroesen *et al.* 2015; Liang *et al.* 2015).

In the adaptive immune system, CD8+ T cells are responsible for recognizing and killing cells infected with viruses and other intracellular pathogens (Butz and Bevan 1998; Williams and Bevan 2007; Joshi and Kaech 2008; Kaech and Cui 2012). Hematopoietic stem cells migrate to the thymus, where they then undergo positive and negative selection to form CD8+ T cells (Starr *et al.* 2003; Schwarz and Bhandoola 2006), which then egress from the thymus and are capable of migrating to sites of infection (Weinreich and Hogquist 2008). CD8+ T cells express different T-cell receptor (TCR) isoforms, thus enabling the CD8+ T cell repertoire to recognize specific antigens. Upon stimulation by a specific and complementary

doi: 10.1534/genetics.115.179176
Manuscript received June 6, 2015; accepted for publication September 18, 2015; published Early Online September 25, 2015.
Available freely online through the author-supported open access option.
Supporting information is available online at www.genetics.org/lookup/suppl/doi:10.1534/genetics.115.179176/-/DC1.
Data in this publication have been deposited in the National Center for Biotechnology Information's Gene Expression Omnibus under accession no. GSE65923.
[1]These authors contributed equally to this work.
[2]Corresponding authors: C5 147 Veterinary Medical Center, Cornell University College of Veterinary Medicine, Ithaca, NY 14853; E-mail: bdr54@cornell.edu; 445 Biotech, Cornell University, Ithaca, NY 14853; E-mail: agrimson@cornell.edu

antigen-presenting cell, a naive CD8+ T cell, which is one that has not previously been activated in response to infection, responds by proliferating and differentiating into cytotoxic effector cells that kill infected cells using proteases and cytolytic proteins (Harty *et al.* 2000). Effector cells are composed of short-lived effector cells (SLECs), which terminally differentiate and undergo apoptosis post-infection, and memory precursor effector cells (MPECs), which can transition into long-lived memory cells that are capable of robustly responding to secondary infection (Kaech *et al.* 2002; Joshi *et al.* 2007; Sarkar *et al.* 2008; Cruz-Guilloty *et al.* 2009; Banerjee *et al.* 2010; Yang *et al.* 2011).

During thymic maturation, CD8+ T cells require the miRNA biogenesis protein Dicer (Muljo *et al.* 2005), and many miRNAs undergo dynamic regulation (Neilson *et al.* 2007). Dicer is also required for *in vivo* activation of mature CD8+ T cells after infection (Zhang and Bevan 2010); in the absence of Dicer, CD8+ T cells neither proliferate nor migrate to sites of infection. Interestingly, Dicer-deficient CD8+ T cells respond more rapidly to *in vitro* stimulation than do wild type (Zhang and Bevan 2010; Trifari *et al.* 2013), suggesting that miRNAs have both activating and inhibitory effects on infection response. Additionally, many miRNAs are differentially expressed during effector and memory cell differentiation (Wu *et al.* 2007; Almanza *et al.* 2010; Trifari *et al.* 2013), some of which have known roles in generating effector cells (Wu *et al.* 2012; Gracias *et al.* 2013; Khan *et al.* 2013; Tsai *et al.* 2013). Importantly, many additional miRNAs with dynamic expression in CD8+ T cells do not have known roles, suggesting that they may also contribute to CD8+ T cell differentiation (Dooley *et al.* 2013; Kroesen *et al.* 2015; Liang *et al.* 2015).

Investigations into roles for miRNAs in lymphocytes have almost exclusively focused on adult cells, although expression of certain miRNAs changes across the life span. For example, miR-181 expression peaks in neonatal CD4+ T cells (Palin *et al.* 2013) and then declines with progressing age, which is important because miR-181 contributes to immune reactivity upon stimulation (Li *et al.* 2012). These data suggest that immune system changes during ontogeny might also be under control of miRNAs. In contrast to CD4+ T cells, nothing is known about the expression patterns and roles of miRNAs in neonatal CD8+ T cells.

Neonatal CD8+ T cells respond to infection profoundly differently than do adult cells (Campion *et al.* 2002; Adkins *et al.* 2003, 2004; Opiela *et al.* 2009; Rudd *et al.* 2013); specifically, neonatal cells proliferate more rapidly in response to primary infection and fail to generate memory cells, thus impairing their response to a secondary infection from the same pathogen (Smith *et al.* 2014). This inability to generate memory cells has important consequences for neonatal health and immunization. Remarkably little is known, however, about the underlying molecular bases that differentiate neonatal and adult CD8+ T cells. Because miRNAs are developmentally regulated (Stefani and Slack 2008; Sayed and Abdellatif 2011; Ebert and Sharp 2012) and are required for the adult CD8+ T cell response, we investigated developmental regulation of miRNAs in CD8+ T cells, motivated to discover if differences in both miRNA expression and regulation by specific miRNAs contribute to the important differences in how differently aged animals respond to primary infection from pathogens. To do so, we examined if miRNAs are differentially regulated between adult and neonatal CD8+ T cells, both before and during primary infection. In parallel, we also defined the mRNA transcriptome in the same sets of cells to identify primary targets of miRNAs as well as other mRNAs that have altered expression in different-aged CD8+ T cells. Surprisingly, our results demonstrate that differential gene regulation between adults and neonates is most pronounced prior to immunological challenge, suggesting that the developmentally regulated miRNAs do not regulate the outcome of effector cells at the peak of the infection response. Instead, these miRNAs may set the activation threshold prior to infection, causing the neonatal CD8+ T cells to differentiate more rapidly into effector cells, thus biasing them toward a terminally differentiated SLEC fate. Multiple lines of evidence implicate miR-29 and miR-130, in particular, as critical regulators of adult and neonatal CD8+ T cells' differential infection responses.

Materials and Methods

Human samples

De-identified whole-adult (18–55 years of age) and cord blood (39–41 weeks gestation) samples, each from three healthy donors, were obtained from New York Blood Center and National Disease Research Interchange, respectively. Mononuclear cells were isolated using Ficoll-paque Plus (GE Healthcare); CD8+ T cells were then isolated using a Naive CD8+ T Cell Isolation Kit (Miltenyi Biotec).

Mice

gBT-I TCR transgenic mice (TCR$\alpha\beta$ specific for SSIEFARL peptide from HSV-1 glycoprotein B498-505) were provided by Janko Nikolich-Zugich (University of Arizona, Tucson, AZ). Ly5.2 mice (8–12 wk) were purchased from the National Cancer Institute (Frederick, MD). Rag$-/-$ OT-I mice were purchased from Taconic (Germantown, NY) and were crossed to C57Bl/6 mice from the National Cancer Institute, and F_1 progeny were used. All pups (male and female) were used for newborn samples (1 day); only male neonatal pups (6–7 days) and adults (2–4 months) were used. Mice were maintained under pathogen-free conditions at Cornell University College of Veterinary Medicine. All experiments were performed in strict accordance with recommendations in the Guide for the Care and Use of Laboratory Animals of the National Institutes of Health; protocols were approved by the Institutional Animal Care and Use Committee (permit no. 2011-0090). All efforts were made to minimize animal suffering.

Naive cells

To isolate naive CD8+ T cells, spleens were harvested from uninfected mice of indicated age groups. Single-cell suspensions

were prepared by mechanical dissociation of spleens through cell strainers. To obtain required numbers of cells, multiple newborn and neonatal spleens were pooled into single samples. CD8+ cells were purified using positive magnetic selection with CD8+ microbeads (Miltenyi Biotec). Following purification, samples were tested for purity, retaining only samples with >90% purity for subsequent sequencing.

Adoptive transfers

Adoptive transfers and infections were performed as described (Smith *et al.* 2014). Briefly, CD8+ T cells were isolated from congenically marked adult and neonatal mice, mixed at a 1:1 ratio, and 2×10^4 cells were transferred intravenously into Ly5.2 recipients. The next day, recipients were intravenously infected with *Lm*-gB (5×10^3 CFU). Effector CD8+ T cells from recipient spleens were isolated with anti-CD8 beads (Miltenyi Biotec) and then sorted via congenic marker expression on a FACS Aria (BD Biosciences).

Thymus isolation

To prepare thymic samples, thymi were collected from mice of indicated ages. Single-cell suspensions were prepared by mechanical dissociation through a cell strainer. Samples were depleted of CD4+ cells by incubating with anti-CD4-biotin followed by magnetic isolation with streptavidin microbeads (Miltenyi Biotec). To specifically isolate single positive CD8+ T cells, CD4− CD8+ Va2+ Vb8+ cells were FACS-sorted to >90% purity with an Aria instrument (BD). Sorted cells were placed in Trizol (Ambion) for extraction of RNA.

Antibodies and flow cytometry

Monoclonal antibodies anti-CD8α (53-6.7), anti-CD4 (GK1.5), anti-CD45.1 (A20), anti-CD45.2 (104), anti-CD90.1/Thy1.1 (OX-7), anti-KLRG1 (2F1), anti-CD127 (A7R34), anti-T-bet (eBio4B10), anti-Eomes (Dan11mag), anti-IL6ST (KGP-130), anti-CD25 (PC61), anti-CD69 (^{1}H.2F3), and anti-CD62L (mel14) were purchased from commercial sources (Biolegend, eBioscience, or Invitrogen). Surface staining was performed by labeling cells for 30 min. Intracellular staining was performed using the Foxp3 staining buffer set (eBioscience). Flow cytometric data were acquired using a FACS LSRII with DiVa software (BD Biosciences) and analyzed with FlowJo (Tree Star).

RNA sequencing

RNA was isolated using Trizol (Life Technologies). One hundred nanograms of total RNA was used to generate small RNA libraries using the NEBNext Small RNA Library kit (NEB) or the TruSeq Small RNA Prep Kit (Illumina). miRNA expression was found with MirDeep2 (Friedländer *et al.* 2012, mm9, miRBase version 21), and differential expression was found with EdgeR (Robinson *et al.* 2010). Approximately 100 ng of total RNA was used to generate mRNA-Seq libraries using the RNA Sample Preparation Kit v2 (Illumina). Reads were aligned to the genome with Tophat (Trapnell *et al.* 2009, mm9), and differential expression was found with CuffDiff (Trapnell *et al.* 2013).

3′-Seq

3′-Seq was performed as described (Lianoglou *et al.* 2013). Briefly, total RNA was poly(A)-selected using a biotinylated poly(T) primer. After complementary DNA synthesis, the RNA was nick-translated and then the ends were cleaned up to allow adapter ligation and PCR amplification. Reads were aligned to the genome with Tophat (Trapnell *et al.* 2009, mm9), and reads whose 3′ ends were near a putative 3′ UTR polyadenylation sequence were quantified.

microRNA targeting

Strong miRNA targets were defined as expressed genes with at least one conserved miRNA target site and a TargetScan (version 6.2) context+ score ≤0.2 (Garcia *et al.* 2011). The background set consisted of any expressed gene that had a conserved miRNA target site with a context+ score ≤0.2 to any broadly conserved miRNA (Friedman *et al.* 2009), excluding all potential targets to the miRNA being tested. Differential targeting between miRNA targets and background were determined using two-sided Kolmogorov–Smirnov tests.

Luciferase assays

HEK293 cells were cotransfected with luciferase reporter plasmids and synthetic miRNAs (IDT) and harvested 24 hr later. Firefly and *Renilla* luciferase activities were measured using Dual-Luciferase Reporter Assay system (Promega) with a Veritas Microplate Luminometer (Turner).

Clustering gene expression data

We clustered expressed genes that were significantly differentially expressed and had at least a twofold difference in expression between adults and neonates in at least one sample [naive, 5, 7, or 15 days post-infection (dpi)]. Those genes were grouped into five clusters using the partitioning around the medoids method (Reynolds *et al.* 2006) in R.

Enrichment statistics

Gene sets were downloaded from the Immunologic Signatures collection at the Molecular Signatures Database (MSDB) (Subramanian *et al.* 2005). We found the number of genes from each data set that belonged to a cluster. For each cluster, we found the number of genes that were located in both the cluster and the data set (b), the total number of genes present in that cluster (n), the number of genes in the MSDB data set (B), and the total number of genes that had been clustered (N). Enrichment was calculated as (b/n)/(B/N). One-sided Fisher exact tests were used to measure significance.

More details regarding the methods are available in Supporting Information, File S1. Data in this publication have been deposited in the National Center for Biotechnology Information's Gene Expression Omnibus (Edgar *et al.* 2002) under GSE65923.

Data availability

Plasmids are available upon request. Supporting information includes naive cell phenotyping (Figure S1), replicate miRNA

expression data (Figure S2), miRNA expression data from CD8+ T cells with a different TCR (Figure S3), replicate mRNA expression data (Figure S4), miRNA targeting (Figure S5), protein expression data (Figure S6), 3′ Seq data (Figure S7), mRNA expression clustering (Figure S8), sorting strategy for thymic cells (Figure S9), mRNA expression of specific effector cell genes (Figure S10), detailed methods (File S1), miRNA expression values (File S2), differences in miRNA family expression (File S3), expression values for miRNA targets (File S4), 3′ UTR isoforms (File S5), mRNA expression values (File S6), and genes present in clusters (File S7). Gene expression data are available at GEO with the accession number: GSE65923.

Results

Neonatal effector CD8+ T cells are predominantly short-lived effectors

Naive CD8+ T cells respond to infection by proliferating and differentiating into cytotoxic effectors that kill infected cells. We previously demonstrated that neonates fail to effectively generate memory CD8+ T cells during primary infection due to cell-intrinsic differences (Smith *et al.* 2014), but the underlying molecular basis remained unknown. Here, we globally identified miRNAs present in neonatal and adult CD8+ T cells, reasoning that one or more miRNAs might contribute to these differences. To focus on cell-intrinsic differences, we eliminated extrinsic differences between adult and neonatal CD8+ T cells in two ways. First, we used CD8+ T cells from adult and neonatal gBT-I mice, which all contain the same TCR (transgenic for HSV-1 glycoprotein $B_{498–505}$, gB), thus ensuring that any differences observed were not due to neonatal animals' smaller TCR repertoire (Rudd *et al.* 2013). Second, we employed an adoptive co-transfer strategy, in which we co-transferred equal numbers of congenic gBT-I CD8+ T cells from adults and neonates into adult recipients, thus ensuring that the adult and neonatal cells were in the same environment. After the co-transfer, the adult recipients were systemically infected with *Listeria monocytogenes* expressing gB (*Lm*-gB). Donor cells were isolated at 5, 7, and 15 dpi using congenic markers (Figure 1A); this strategy allowed us to capture key events during the CD8+ T cell response to primary infection: expansion, peak response, and contraction, respectively. Consistent with previous findings (Smith *et al.* 2014), neonatal cells responded vigorously during expansion but were outnumbered by their adult counterparts on days 7 and 15 (Figure 1B). The neonatal effector cell population was predominantly composed of SLECs ($KLRG1^{hi}IL7R^{lo}$), whereas adults generated many more MPECs ($KLRG1^{lo}IL7R^{hi}$), a difference that was observed at all three time points (Figure 1, C and D).

To establish that uninfected neonatal CD8+ T cells possess characteristics of naive cells equivalent to those of adults, we monitored several proteins whose expression patterns differentiate between naive and effector cells. We first found that adult and neonatal naive cells have equivalently high levels of the naive cell marker SELL/CD62L, which controls lymph homing (Figure 1E). Additionally, we found that adult and neonatal naive CD8+ T cells have similarly low levels of markers associated with activation (IL2RA/CD25 and CD69, Figure 1E). Finally, we measured KLRG1 and IL7R expression to determine if expression differences seen during infection are present prior to infection; however, adult and neonatal cells were similarly $KLRG1^{lo}IL7R^{hi}$ (Figure 1E). Together, these results demonstrate that neonatal CD8+ T cells have naive characteristics prior to infection. Importantly, we also determined that our method for isolating CD8+ T cells for the adoptive cotransfer did not activate the cells, as demonstrated by cells before and after selection having equivalent expression of SELL, IL2RA, CD69, KLRG1, and Il7R (Figure S1).

Neonatal and adult CD8+ T cells from naive mice have pronounced differences in miRNA expression

MicroRNAs have been implicated in controlling adult naive CD8+ T cell differentiation into SLECs or MPECs (Liang *et al.* 2015); thus, we hypothesized that differential miRNA expression between adult and neonatal effector CD8+ T cells contributes to the lack of MPECs in neonates. We used high-throughput sequencing to profile miRNAs present in adult and neonatal CD8+ T cells at 5 and 7 dpi (as shown in Figure 1A).

CD8+ T cells had 47 miRNA families that were well expressed [>1000 reads per million (RPM)] under at least one condition (File S2). MicroRNA families consist of miRNAs with identical or near identical targeting properties (Lewis *et al.* 2003). When we compared the miRNA profiles across all samples, we were surprised to find highly similar patterns of miRNA expression between neonatal and adult effector cells at both 5 and 7 dpi. Such similarities were observed using principal component analysis (PCA) (Figure 2A) and fold-change differences in expression (Pearson $r > 0.99$, $P < 10^{-15}$, Figure 2B). Moreover, we found no miRNAs with statistically significant differential expression between adult and neonatal effector cells at either time point (Figure 2B and File S3). Interestingly, despite the pronounced difference in the SLEC:MPEC ratio between adults and neonates (Figure 1D), their highly concordant miRNA profiles suggested that SLECs and MPECs themselves possess extremely similar miRNA profiles.

We next profiled miRNAs from purified naive CD8+ T cells. In contrast to effector cells, miRNA expression differed greatly between naive neonatal and adult cells (Figure 2, A and B), including significant differential expression of 10 of the 47 well-expressed miRNA families. Many of the differentially expressed miRNAs have been implicated in CD8+ T cell processes. For example, miR-130 is upregulated in adult CD8+ T cells in early infection and is associated with T-cell activation (Zhang and Bevan 2010); it is also upregulated in neonatal naive CD8+ T cells (Figure 2B). Conversely, miR-29, miR-146, and miR-150, which are downregulated in naive neonatal CD8+ T cells (Figure 2B), are implicated as negative regulators of CD8+ T-cell infection response (Ma *et al.* 2011; Yang *et al.* 2012; Trifari *et al.*

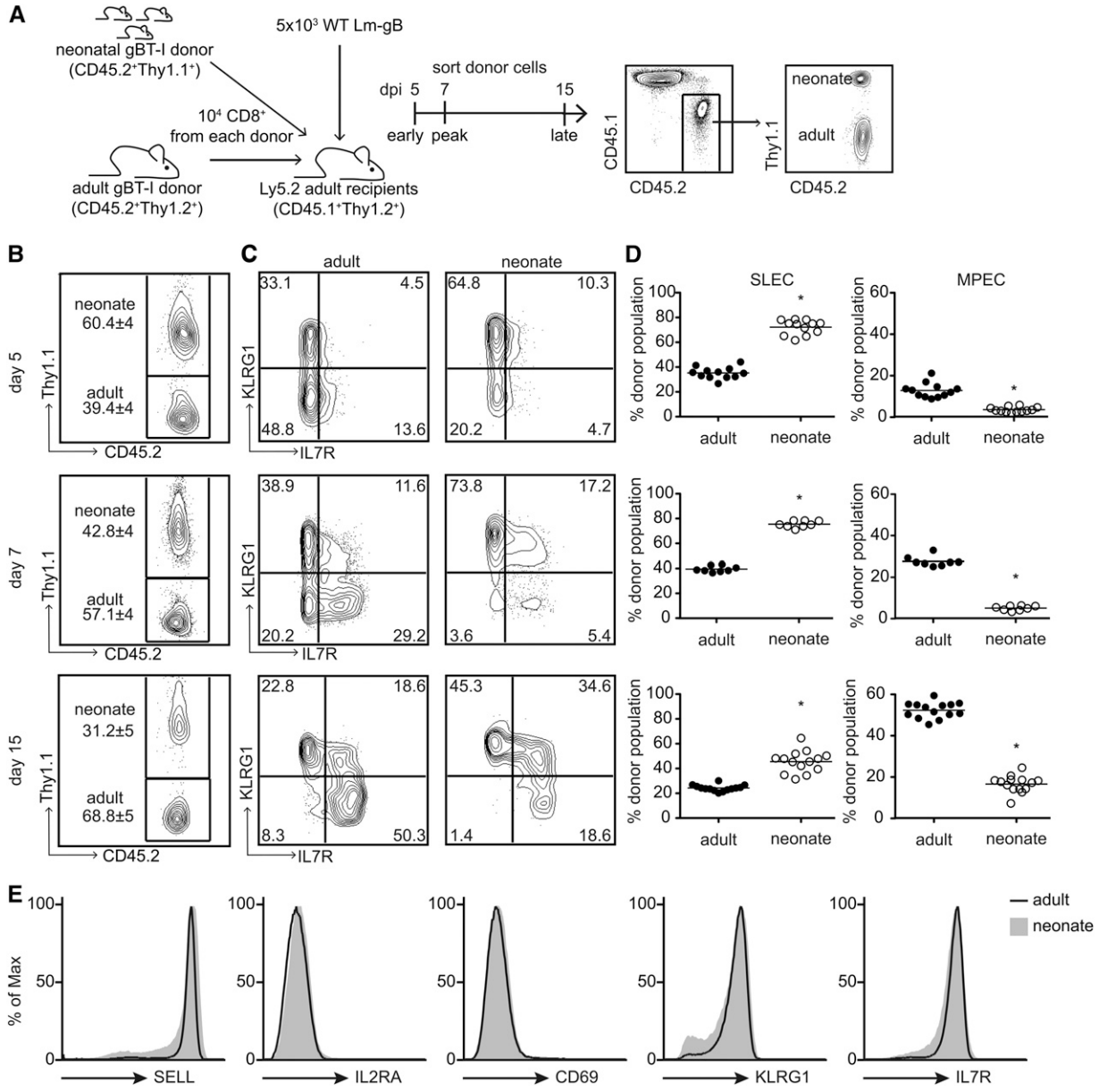

Figure 1 Phenotypic differences between adult and neonatal CD8+ T cells. (A) Schematic of experimental strategy. Congenically marked adult (CD45.2+Thy1.2+) and neonatal (CD45.2+Thy1.1+) donor gBT-I CD8+ T cells (1×10^4) were transferred intravenously into wild-type congenically marked adult recipients (CD45.1+Thy1.2+), which were infected with *L. monocytogenes* expressing gB peptide. At 5, 7, and 15 dpi, spleens were harvested and donor cells sorted by flow cytometry based on congenic marker expression. Sorted cells were used for all downstream cellular and molecular assays performed on effector cells. (B–D) Distinguishing and quantifying both adult *vs.* neonatal and SLEC *vs.* MPEC CD8+ T cells in recipient animals. (B) Representative contour plots showing percentages (±SD) of adult and neonatal donor cells at 5, 7, and 15 dpi. The amount of Thy1.1 produced by CD45.2+ donor cells was used to differentiate adult (Thy1.1−) and neonatal (Thy1.2+) cells. (C) Representative contour plots of KLRG1 *vs.* IL7R for adult and neonatal donor cells at 5, 7, and 15 dpi. (D) Statistical analysis of SLEC ($KLRG^{hi}IL7R^{lo}$) and MPEC ($KLRG1^{lo}IL7R^{hi}$) populations at 5, 7, and 15 dpi. Significance was determined by paired *t*-test; $*P < 0.0001$. Data are representative of two experiments (n = 8–12 mice/group). (E) Representative histograms show expression of SELL, IL2RA, CD69, KLRG1, and IL7R of adult and neonatal CD8+ cells after positive selection.

2013). These results identify differential miRNA expression in naive cells as a possible basis for the altered behavior of neonatal and adult CD8+ T cells after infection.

To further explore developmental differences in miRNA expression, we profiled naive CD8+ T cells from newborn mice (1 day old). Differences in the global miRNA profile between newborn and adult naive cells were highly similar to differences that we observed between neonates and adults; such differences, however, were more pronounced in newborn mice than in neonates (Figure 2, A and B, $P < 0.05$). Together, these results show that the naive miRNA profile is largely age-dependent in CD8+ T cells.

To confirm that the age-dependent differences in miRNA expression that we observed (Figure 2) are not specific to a

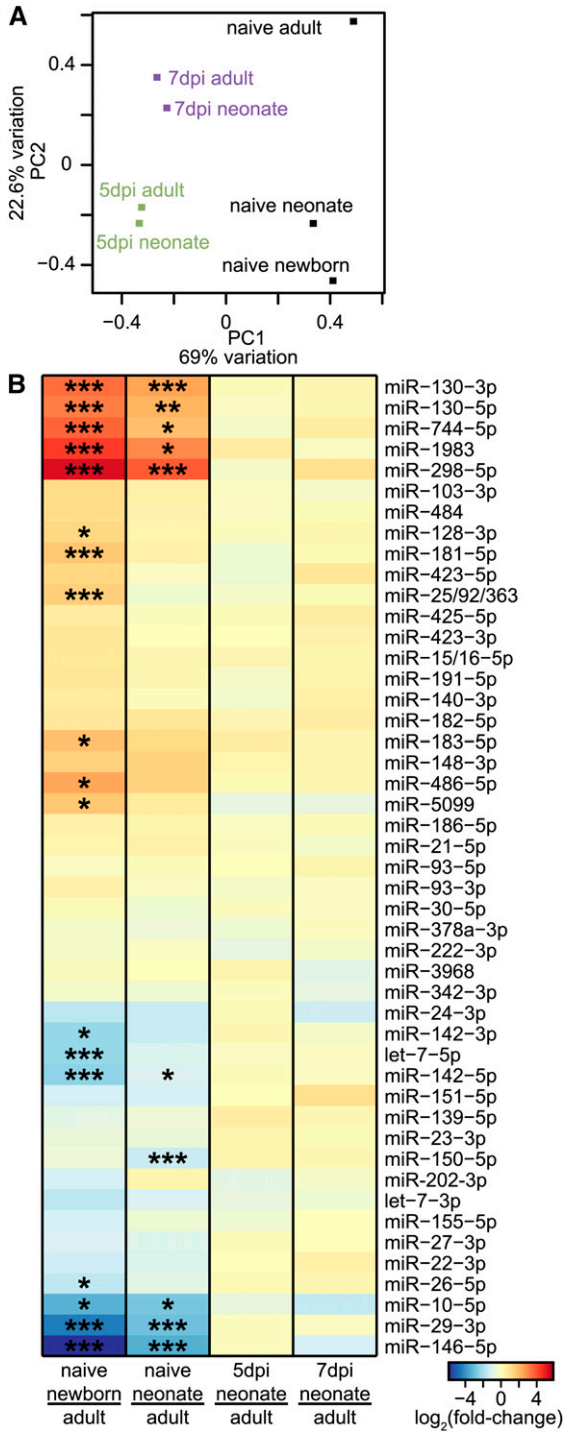

Figure 2 Differential microRNA expression in adults and neonates. (A) PCA using RPM values of well-expressed miRNAs. Adult and neonatal naive samples consist of two highly correlated pooled biological replicates (Figure S2); naive newborn and 5- and 7-dpi samples each consist of one replicate. The percentage of the overall variation accounted for by principal components 1 (*x*-axis) and 2 (*y*-axis) is indicated for each axis. (B) Fold-change difference in expression between adults and neonates was found for miRNA families in naive and 5- and 7-dpi CD8+ T cells, as well as between naive adult and newborn cells. Reads for miRNAs corresponding to the same family were summed. Significance was determined by edgeR exact test with multiple test correction (Benjamini–Hochberg; $*P < 0.05$, $**P < 0.005$, $***P < 0.0005$). Small RNA expression data were replicated with independent biological samples, using an alternative method of sequencing library construction (see Figure S2).

particular CD8+ TCR transgenic mouse line (gBT-I mice), we repeated our miRNA profiling in adult, neonatal, and newborn naive CD8+ T cells isolated from another transgenic T-cell mouse line (OT-I mice), which expresses a CD8+ TCR specific to the OVA peptide SIINFEKL. Importantly, the age-dependent miRNA expression differences observed in gBT-I CD8+ T cells were recapitulated well in OT-I CD8+ T cells (Figure S3), demonstrating that these differences in naive CD8+ T cell miRNA expression are robust across two different mouse genetic backgrounds.

Identification of conserved expression differences in developmentally regulated miRNAs

To determine if age-related miRNA expression differences are conserved in humans, we profiled miRNAs present in naive human CD8+ T cells from adult peripheral blood and from cord blood, which is developmentally similar to murine neonatal blood (Adkins *et al.* 2004). Fold-change expression differences between adult and neonatal cells correlated significantly between mice and humans for the 55 miRNA families that were well expressed in either one or both species (Figure 3). Of the 10 miRNAs with significant differential expression between adult and neonatal CD8+ T cells in mice, three had equivalent expression differences in humans: miR-29, miR-130, and miR-150. These particular miRNAs, therefore, are most likely to have conserved biological functions in CD8+ T cells.

Targets of miR-29 and miR-130 differ in expression between adults and young mice

MicroRNAs affect phenotypes via repression of mRNA targets, yet changes in miRNA expression do not necessarily cause differential target regulation because only miRNAs expressed at high levels are able to mediate a detectable impact upon the transcriptome. Moreover, our understanding of miRNAs is insufficient to predict the consequences of modest changes in their expression levels (Bartel 2009; Mukherji *et al.* 2011). We therefore measured the effects of well-expressed miRNAs in differently aged naive CD8+ T cells by comparing the changes in expression for targets of well-expressed miRNAs between adults and neonates/newborns using RNA-Seq. For each sample, we sequenced at least two biological replicates, which were highly correlated for all samples (Figure S4).

We predicted targets using TargetScan for each of the miRNA families that are well expressed in murine CD8+ T cells (Friedman *et al.* 2009; Garcia *et al.* 2011). To determine if a miRNA's targets had altered expression in naive CD8+ T cells, we found the expression difference for those targets, individually comparing both newborns and neonates to adults, and then compared those values to a background set of genes targeted by other miRNAs. Only four miRNA families had significant differential targeting between adults and newborns, and three of those were also different between adults and neonates ($P < 0.05$, Figure 4A). Three of the miRNAs exhibiting

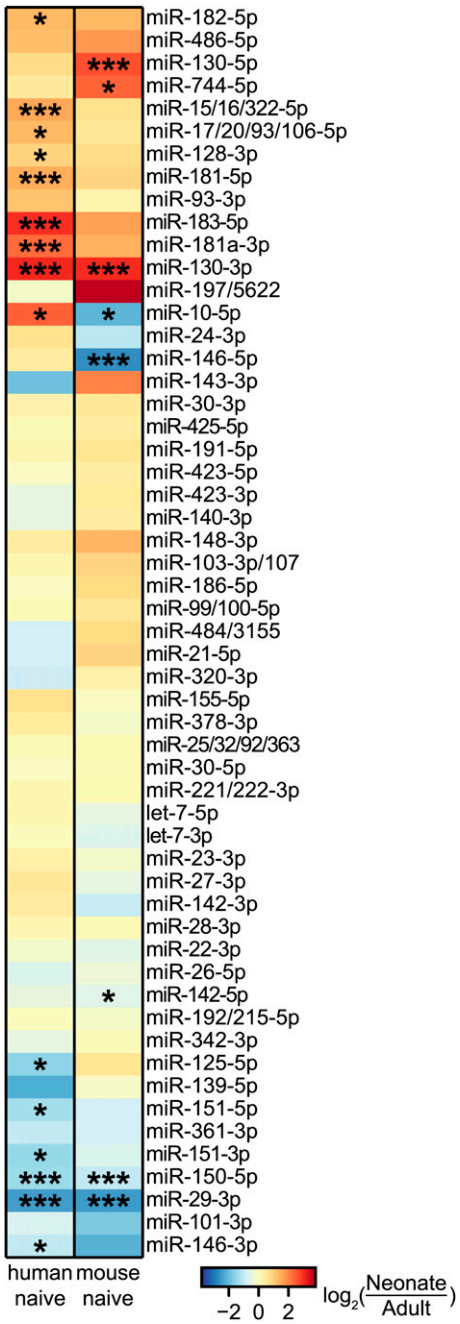

Figure 3 MicroRNA expression in naive human cells. Fold-change differences in expression were calculated comparing adults and neonates for miRNAs well expressed in humans and/or mice. Mice samples consist of two pooled biological replicates; human samples consist of three pooled biological replicates. $*P < 0.05$, $***P < 0.0005$.

differential targeting were themselves significantly differentially expressed; as expected, target sets had reciprocal expression to their cognate miRNAs. Notably, two of these miRNAs, miR-29 and miR-130, correspond to those with conserved expression differences in human adult and neonatal CD8+ T cells (Figure 3).

The miRNA miR-29 is downregulated in newborn and neonatal CD8+ T cells, while its mRNA targets are more highly expressed in those cells (Figure 4B). Conversely, miR-130 is upregulated in newborn and neonatal CD8+ T cells, while its targets are more lowly expressed in those cells (Figure 4C). These targeting differences were robust to analyses using different background gene sets (Figure S5). Importantly, targets of both miRNAs that were predicted to be stronger exhibited more pronounced differences in their expression between adults and neonates when compared to those predicted to be weaker, strongly suggesting that differential expression of these miRNAs is directly controlling their targets' expression (Figure S5).

Predicted targets are repressed by miR-29 and miR-130

We next investigated the differentially expressed targets of miR-29 and miR-130 (File S4) that had established roles in adult CD8+ T cell function. Notably, targets of miR-29 include *Eomes* and *Tbx21* (T-bet), both of which encode transcription factors that upregulate genes required for effector function (Intlekofer *et al.* 2005; Banerjee *et al.* 2010; Kaech and Cui 2012). The transcripts of *Eomes* and *Tbx21* were significantly upregulated in naive neonates and newborns, as compared to adults (Figure 4D); importantly, we confirmed this upregulation for both proteins in neonates (Figure 4, E and F; Figure S6). Targets of miR-130 include the transcription factor *Irf1*, which is required for CD8+ T cell development in the thymus (Penninger *et al.* 1997), and the chemokine receptor *Il6st*, which has been suggested to protect effector cells from apoptosis at the resolution of the CD8+ T cell response (Castellino and Germain 2007). Both *Irf1* and *Il6st* transcripts are downregulated in newborn and neonatal mice; although we were unable to test IRF1 protein levels, we confirmed this downregulation for the IL6ST protein in neonates (Figure 4, D and G; Figure S6).

Because miRNA target prediction is imperfect, we used reporter assays to investigate whether targets were correctly predicted. Portions of the putative targets' 3′ UTRs containing the miRNA target sites were placed downstream of a luciferase reporter; the target site was disrupted via mutagenesis to generate a paired control incapable of repression by the cognate miRNA. After cotransfecting each reporter with either miR-29 or miR-130, we compared differences in luciferase activity between the intact and disrupted target sites. Target sites in *Eomes* and *Tbx21* were specifically repressed by miR-29, whereas sites in *Irf1* and *Il6st* were specifically repressed by miR-130 (Figure 4H). These results, together with *in vivo* mRNA and protein quantifications (Figure 4, D–G), indicate that these genes are likely true targets of their respective miRNAs.

Mammalian 3′ UTRs are often alternatively processed to generate multiple isoforms to regulate gene expression (Mayr and Bartel 2009; Lianoglou *et al.* 2013), in part by changing the available miRNA target sites (Sandberg *et al.* 2008; Nam *et al.* 2014). We used 3′-Seq (Lianoglou *et al.* 2013), a technique that globally sequences the 3′ termini of mRNAs, to investigate alternative 3′ UTR processing in naive adult and neonatal CD8+ T cells. Most transcripts primarily

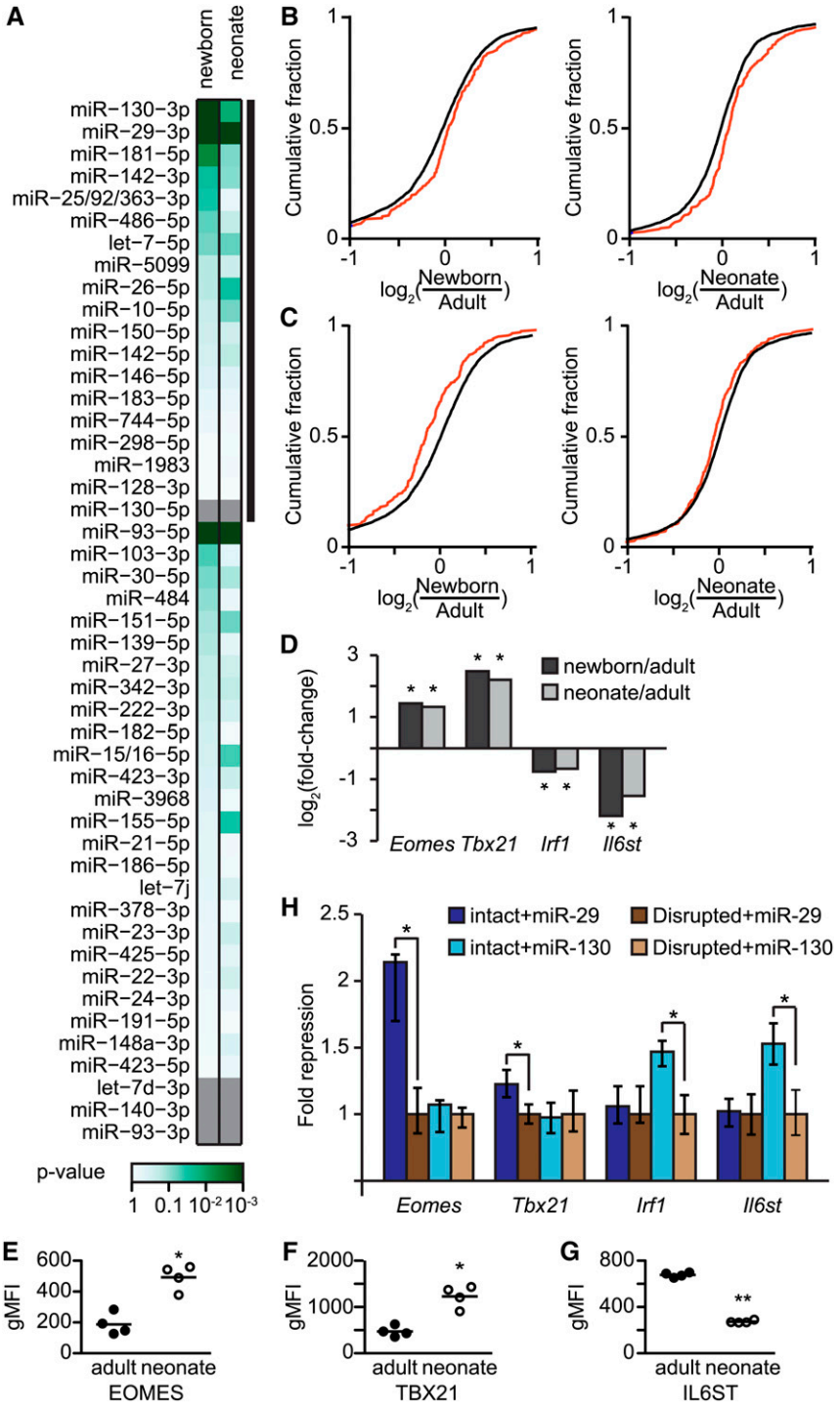

Figure 4 miRNA targets. (A) Significant differences in miRNA target expression. Fold-change differences in expression between adults and neonates (or newborns) were found for predicted targets of each miRNA expressed in CD8+ T cells, which were then compared to fold changes in expression of a background set. Differentially expressed miRNAs are indicated with a thick black line, and miRNAs without predicted targets are shown in gray. Significance was determined by Kolmogorov–Smirnov tests. All samples consist of two pooled biological replicates; see also File S4. (B and C) Cumulative fold-change differences in expression of newborns (left) and neonates (right) compared to adults is shown for background genes (black) and targets (red) of miR-29 (B, $P < 10^{-4}$) and miR-130 (C, $P < 0.05$). Expression values for targets are the mean Fragments Per Kilobase of transcript per Million mapped reads (FPKM) values of two pooled biological replicates. (D) Mean differences in expression for neonate or newborn FPKM value compared to the adult value. Benjamini–Hochberg corrected significant differential expression was determined using CuffDiff. $*P < 0.05$ (E–G) Differences in protein expression between naive adult and neonatal samples as determined by flow cytometry for EOMES (E), TBX21 (F), and IL6ST (G). Significance determined by unpaired *t*-test, $*P < 0.01$, $**P < 0.0001$; see also Figure S6. (H) Fold repression of putative miRNA targets. The luciferase activity of reporter constructs containing intact miRNA target sites was normalized to otherwise identical reporters with disrupted target sites in the presence of miR-29 or miR-130. Reporter data plotted as fold repression (*y*-axis) of reporters with intact sites relative to those with disrupted sites. Data are represented as the geometric mean ± 33% of the spread of the data; $n = 12–18$; significance was determined by a two-sided Wilcoxon rank-sum test; $*P < 0.0005$.

express one 3′ UTR isoform; some genes (33%) express multiple isoforms, suggesting that different miRNA target sites might be present (Figure 5A). To determine if 3′ UTR isoform usage altered miR-29 and miR-130 targeting, we repeated our targeting analysis using the isoforms present in naive cells (File S5). Most predictions were unaffected, and adults and neonates almost always (~90%) use the same 3′ UTR isoform in naive CD8+ T cells, resulting in the same miRNA target site availability for miR-29 and miR-130 (Figure 5, B and C; Figure S7). Specifically, we found that isoforms for *Eomes*, *Tbx21*, *Irf1*, and *Il6st* contain the expected miRNA targets sites, and importantly, isoform preference was equivalent in adults and neonates; *Cd69* was also included as a likely target of miR-130 (Zhang and Bevan 2010). We found two *Eomes* 3′-UTR isoforms, one containing a single miR-29 target site and the other a pair of sites; however, relative usage of the isoforms was unchanged between adult and neonatal CD8+ T cells (Figure 5D). These results indicate

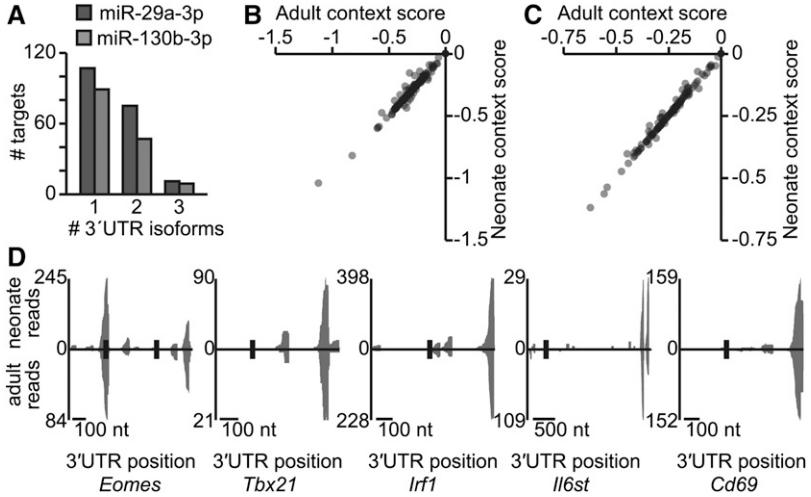

Figure 5 3′ UTR isoforms in naive CD8+ T cells. (A) The number of 3′-UTR isoforms expressed in adult and neonatal naive cells for miR-29 and miR-130 targets, as determined by 3′ Seq. The naive adult data are derived from two pooled biological replicates; the naive neonate has one replicate; see also File S5. (B and C) Isoform-weighted context scores for predicted targets of miR-29 (B) and miR-130 (C), comparing adult and neonatal samples (Pearson correlation coefficients > 0.98; $P < 10^{-15}$ for targets of both miR-29 and miR-130). Context scores were weighted by the percentage of isoforms that contain each miRNA target; see also Figure S7. (D) Gene models shown with miRNA target sites in black, and density of 3′ Seq reads corresponding to 3′ termini of different isoforms.

that the differential miRNA targeting observed between adult and neonatal naive CD8+ T cells is not complicated by 3′-UTR isoform usage and further indicate that *Eomes*, *Tbx21*, *Irf1*, and *Il6st* are likely regulated by miR-29 or miR-130 *in vivo*.

Global differences in adult and neonatal CD8+ T-cell transcriptomes are pronounced in naive cells

Our results identify miR-29 and miR-130 as developmentally regulated miRNAs in differently aged naive CD8+ T cells in both mice and humans. Importantly, their targets include genes whose functions are known to affect differentiation into SLECs and MPECs. MicroRNAs exert their cumulative effects not only by repression of their direct targets, but also from resulting downstream expression differences due to target repression, creating indirect miRNA targets. Thus, the overall age-related transcriptome differences in CD8+ T cells are derived from direct and indirect effects of miRNAs, together with additional differences not attributed to miRNAs. We therefore systematically investigated age-related expression differences in CD8+ T-cell transcriptomes of adults, neonates, and newborns.

Global transcriptome differences were visualized using PCA (Figure 6A) and pairwise similarity between samples (Figure 6B), both of which indicate large transcriptomic differences in response to infection but smaller differences between adults and neonates at each time point; for naive cells, neonatal gene expression is more similar to newborns than to adults. Additionally, nearly 10 times more genes were significantly differentially expressed between adults and neonates in naive cells than in any stage of effector cells. Moreover, newborn naive CD8+ T cells have more differentially expressed genes with adults than do neonates (Figure 6C and File S6). Thus, similar to the age-dependent changes that we observed in miRNA expression (Figure 2A), we found that the CD8+ T-cell transcriptome also exhibited the most pronounced age-dependent changes in naive cells, rather than effector cells at any stage of the primary immune response.

Genes with similar changes in expression are often co-regulated and tend to possess similar biological functions (D'haeseleer 2005). Using unsupervised clustering, we found four groups of genes that have differential expression between adult and either neonatal or newborn CD8+ T cells (Figure 6D and File S7). The more modest differences between adult and neonatal effector cells were masked by the large expression differences in naive cells. Clusters 1 and 4 contain genes that are upregulated in adult CD8+ T cells, whereas clusters 2 and 3 show upregulation in the newborns and neonatal cells. To potentially detect expression differences in effector cells, we omitted the newborn expression data while performing the clustering; the differences in naive cells were still far larger than those at 5, 7, or 15 dpi (Figure S8). This clustering analysis further demonstrates that the age-related differences in gene expression in naive cells are far more extreme than those detected in effector cells. Taken together with our miRNA profiling, these analyses strongly suggest that the differences that exist between adult and neonatal CD8+ effector T cells are likely established in naive cells prior to infection and differentiation into effector cells.

To gain perspective on the possible biological functions of co-regulated clusters, we cross-referenced each cluster with curated gene sets that define and differentiate SLECs, MPECs, naive, effector, and memory cells (Kaech *et al.* 2002; Subramanian *et al.* 2005; Joshi *et al.* 2007). We found that both clusters 1 and 2 significantly overlap with certain of the curated gene sets. Cluster 1, which is downregulated in naive neonates and newborns, is significantly enriched for genes that distinguish naive from effector cells, memory from effector cells, and MPECs from SLECs. Taken together, these results suggest that, compared to naive adults, cells from both neonates and newborns have a lower expression of genes that defines naive and memory cells. Cluster 2, which is upregulated in naive neonates and newborns, is enriched in genes that distinguish effector cells from both naive and memory cells (Figure 6E). Importantly, for both clusters 1 and 2, the observed differences in gene expression were present only in naive cells, and not in effector cells. Together, these results demonstrate that, prior to infection, neonatal and newborn CD8+ T cell transcriptomes already begin to resemble those of effector cells, suggesting

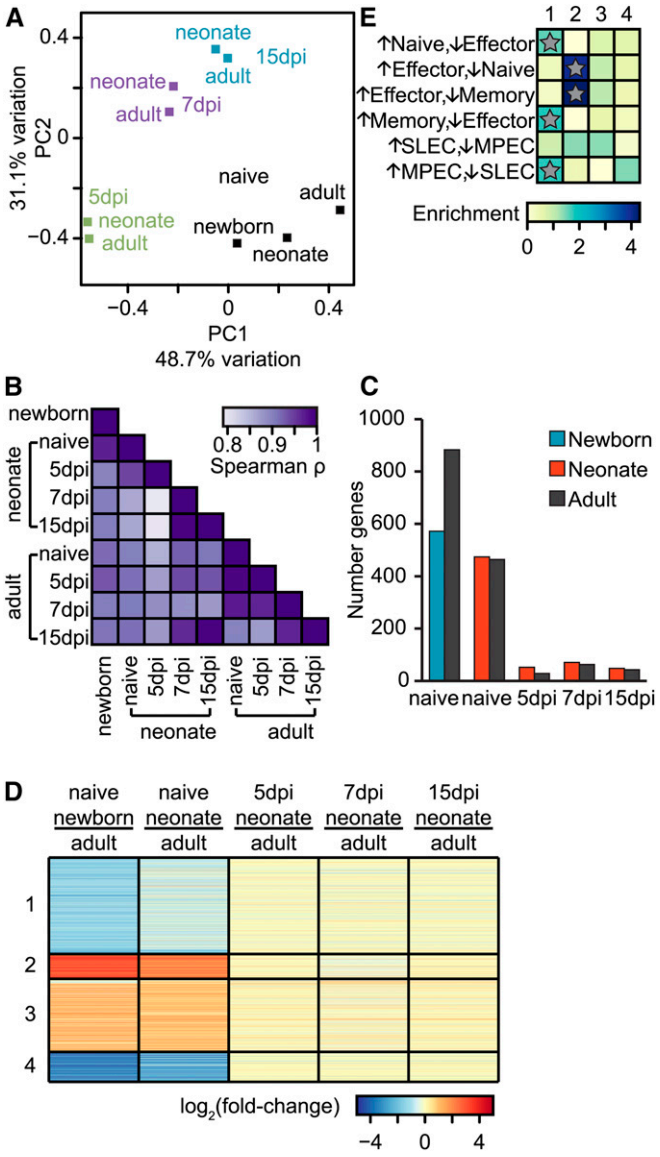

Figure 6 Differential gene expression in adult and neonatal CD8+ T cells. (A) PCA comparing naive and effector CD8+ T cells from different developmental stages. PCA, and all subsequent analyses (B–F), were performed on genes with an FPKM > 1 in at least one sample. The mean FPKM value was found for each sample, and PCA was performed on log-transformed values. The percentage of the overall variation accounted for by principal components 1 (*x*-axis) and 2 (*y*-axis) is indicated for each axis. (B) Color-coded pair-wise Spearman rank correlation coefficients comparing transcriptomes between different samples; $P < 10^{-15}$ for all comparisons. (C) Number of genes that exhibited differences in expression that is at least twofold and significant (Benjamini–Hochberg corrected *P*-value <0.05) between pairs of samples. For naive and 5-, 7-, and 15-dpi samples, we compared adults and neonates; for naive, we additionally compared adults and newborns. See also File S6. (D) Clustering of co-regulated genes in newborn, neonatal, and adult CD8+ T-cell transcriptomes. Fold-change differences for all genes represented in B were calculated between adults and neonates or newborns. Clustering was performed to identify genes with similar changes in expression throughout infection; fold change for each gene is plotted in each sample, and genes are shown in their clusters; see also File S7. (E) Genes in each cluster were compared to genes that define naive, effector, memory, MPEC, or SLEC cells. Enrichment was calculated as the number of genes in each cluster as compared to the number expected. Significance was determined by Fisher exact tests; $*P < 10^{-4}$.

that this effector-like gene expression lowers the activation threshold of naive neonatal CD8+ T cells.

MicroRNA profiles in the thymus resemble neonatal naive cells

The underlying causes of the age-related differences in CD8+ T-cell miRNA expression that we have described are likely complex and due to developmental differences between adults, neonates, and newborns. CD8+ T cells are derived from hematopoietic stem cells (HSC) that undergo differentiation in the thymus. After exiting the thymus, CD8+ T cells are not yet fully mature; they undergo additional development for 3 weeks after their thymic emigration (Berzins *et al.* 1998). Stem cell origin is one possible basis for differential expression of miRNAs: CD8+ T cells of neonates and newborns are derived from fetal liver HSCs, whereas those of adults are derived from bone marrow HSCs (Jotereau *et al.* 1987; Foss *et al.* 2001). Alternatively, differences in cellular maturity might contribute to differential expression of miRNAs; neonatal and newborn naive cells are composed of less mature cells that have recently exited the thymus, whereas ~80% of adult cells have undergone complete post-thymic maturation (Hale *et al.* 2006; Fink 2013). Importantly, these models are not mutually exclusive; moreover, the extent to which each model contributes may differ for specific miRNAs. To distinguish between these models, we compared the miRNA profiles of naive CD8+ T cells (located in the spleen) to those of immature adult, neonatal, and newborn CD8+ T cells found in the thymus (Figure S9). If age-dependent differences in miRNA expression are caused by HSC origin, adult and newborn thymic CD8+ T cells will have miRNA differences that mirror those differences observed in adult and neonatal/newborn splenic CD8+ T cells. It is worth noting that the miRNA profiles of neonatal thymic cells may be less informative as they are likely composed of both HSC populations. Alternatively, if the differences in miRNA profiles are instead due to time spent in the periphery, where additional post-thymic maturation occurs, neonatal and newborn splenic miRNA expression will more closely resemble that of thymic samples from all ages, which together will be distinct from miRNA expression found in the adult spleen.

We first globally compared the expression of all well-expressed miRNAs by using pair-wise similarities between the samples (Figure 7A). When we compared miRNA profiles between thymus-derived samples, the profiles differed according to the age of the animal, suggesting that HSC origin contributes, at least to a degree, to differential regulation of miRNAs. Overall, however, the thymus profiles from all samples more closely resemble splenic neonatal and newborn profiles than that of the splenic adult. This result implies that the major determinant of the overall miRNA profile corresponds to the amount of time that CD8+ T cells have spent out of the thymus. Notably, these same patterns were also evident when we focused on only the expression of miRNAs identified previously as differentially expressed in naive cells (Figure 2B): patterns in thymic samples were more similar to

those of neonatal and newborn splenic samples than to the profile found in the adult spleen, which possesses the most distinct profile of all the samples (Figure 7B).

Importantly, some miRNAs were expressed relatively uniformly in the thymus, independent of age, whereas others varied by age (Figure 7B); this result indicated that changes in expression of different miRNAs do not all share a common basis. Because our previous data implicate miR-29 and miR-130 as miRNAs associated with age-dependent changes in CD8+ T-cell phenotypes, we specifically examined their expression in the thymus-isolated and spleen-isolated naive CD8+ T cells (Figure 7C). Levels of miR-29 in the immature thymus-derived cells are low, regardless of the age of the animal and thus HSC lineage, indicating that control of miR-29 expression is likely primarily determined by maturation after egress from the thymus. Specifically, levels of miR-29 are highest in the adult spleen, which contains CD8+ T cells that are more mature than any of the other conditions that we examined. For miR-130, the upregulation in neonates and newborns when compared to adults is mirrored in the thymus, which implicates HSC origin as a major factor controlling levels of miR-130. Levels of miR-130, however, were different when the two adult samples were compared: miR-130 only reaches its lowest levels in the adult spleen, which indicates that the maturation status of CD8+ T cells also correlates with control of miR-130. These data imply that both HSC origin and post-thymic maturation influence control of miR-130 levels. Together, these data demonstrate that one model alone does not explain differences in splenic adult and neonatal immunity. While miRNA expression in thymic adult CD8+ T cells closely resembles that found in thymic neonates and newborns, indicating that post-thymic cellular maturation is a major determinant of miRNA profiles in CD8+ T cells, the expression of some miRNAs appears to be due also to HSC origin.

Discussion

Here, we show that adult and neonatal CD8+ T cells have highly similar gene expression profiles during primary infection despite large phenotypic differences. Instead, the greatest differences between adults and neonates are found in naive cells in mRNA and especially miRNA expression profiles. Downstream targets of the differentially expressed miRNAs miR-29 and miR-130 include the chemokine receptor *Il6st* and the transcription factors *Irf1*, *Eomes*, and *Tbx21*. These results suggest that regulatory differences in naive cells underlie neonates' inability to create memory cells during infection, and they identify miR-29 and miR-130 as potential factors that contribute to establishment of these differences.

After primary microbial challenge, naive adult CD8+ T cells differentiate into SLECs and MPECs, whereas neonates primarily differentiate into SLECs. We were therefore surprised that the adult and neonatal effector miRNA profiles were more similar to each other than to cells at differing infection stages. These results suggest that miRNA expression differences previously seen between SLECs and MPECs (Khan *et al.* 2013) were relatively minor, especially when compared to the far greater differences that we observed between adult and neonatal/newborn naive cells. Another possibility is that SLECs produce vastly more miRNAs than MPECs, or vice versa, and thus the miRNAs from one cell type might dominate the overall profile. Regardless, phenotypic differences in adult and neonatal immunity are not explained by miRNA expression during infection.

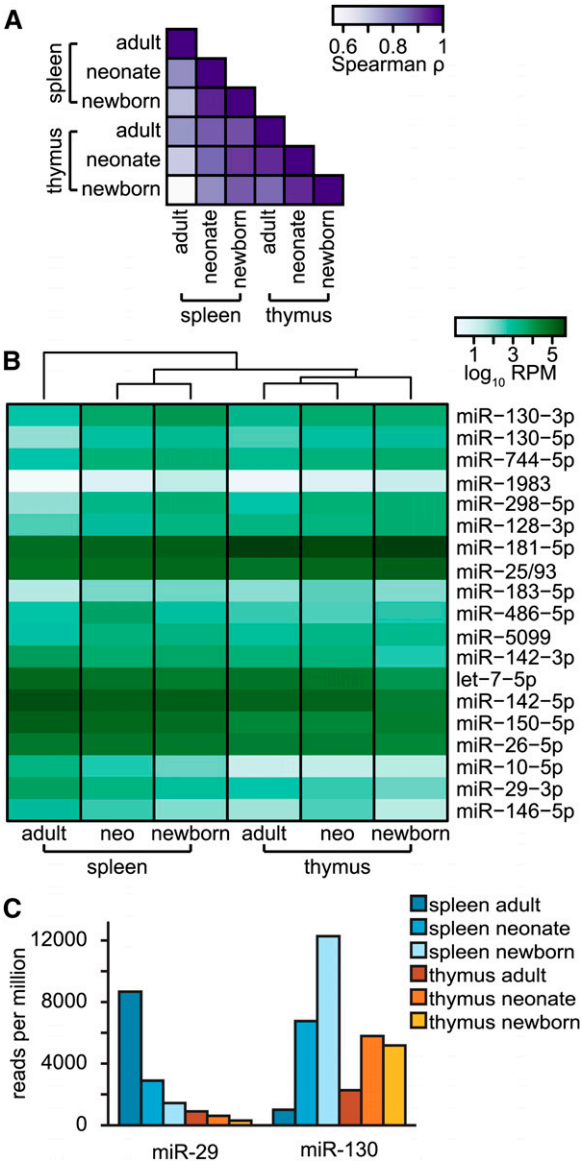

Figure 7 MicroRNA expression in immature and mature CD8+ T cells. (A) Color-coded pair-wise Pearson correlation coefficients comparing miRNA RPM values for adult and neonatal CD8+ T cells derived from the spleen and thymus. All adult samples and neonatal thymus samples are derived from two pooled biological replicates; the remaining samples consist of one biological replicate. See also Figure S9 and File S2. (B) Expression, in RPM, is shown for miRNAs that are significantly differentially expressed between naive adult cells as compared to neonatal and newborn cells (in the same order as Figure 2B). The samples were ordered via Euclidean clustering. (C) RPM values for miR-29 and miR-130 expression levels are shown for all samples.

MicroRNAs miR-29 and miR-130 are of particular interest because gBT-I mice, OT-I mice, and humans show consistent expression differences between adults and neonatal naive CD8+ T cells. miR-29 is highly expressed in adult naive cells; importantly, downregulation of miR-29 upon activation is necessary for efficient cell killing, and mice that lack miR-29 are more resistant to infection than wild type (Ma *et al.* 2011). Thus, naive neonates' lowered miR-29 expression resembles that of adults post-activation, suggesting that neonatal naive cells more easily undergo activation, which primes them for effector functions. Conversely, miR-130 is upregulated shortly after activation in adult cells, and its expression correlates with the cells' ability to exit lymphoid organs (Shiow *et al.* 2006; Zhang and Bevan 2010). Naive neonatal expression of miR-130, therefore, also resembles that of adult effector cells. Increased neonatal miR-130 in naive cells might allow the cells to more quickly reach sites of inflammation after activation, thereby promoting SLEC differentiation (Joshi *et al.* 2007; Sarkar *et al.* 2008; Gerlach *et al.* 2010; Jung *et al.* 2010). Thus, changes in miR-29 and miR-130 expression in naive neonates are consistent with rapid acquisition of effector functions and may allow neonates to compensate for smaller repertoires of CD8+ T cells in early life (Rudd *et al.* 2011, 2013).

We demonstrated that miR-29 can directly repress *Tbx21* and *Eomes*, which encode partially redundant transcription factors that upregulate genes needed during infection, such as *Ifng*, *Cxcr3*, and *Il2rb* (Intlekofer *et al.* 2005; Banerjee *et al.* 2010), each of which is significantly upregulated in naive neonatal cells (Figure S10). Expression of *Tbx21* and *Eomes* is low in adult naive cells, and their upregulation during infection is driven by external cell signaling (Takemoto *et al.* 2006; Joshi *et al.* 2007; Cruz-Guilloty *et al.* 2009; Pipkin *et al.* 2010; Rao *et al.* 2010, 2012; Kaech and Cui 2012). Therefore, lowered expression of miR-29 in neonatal naive cells likely directly results in elevated expression of *Tbx21* and *Eomes*, which facilitates upregulation of effector-function proteins prior to infection. Thus, upregulation of *Tbx21* and *Eomes* may be one specific mechanism by which decreased miR-29 expression in naive neonatal cells promotes a SLEC fate.

Importantly, our data suggest that age *per se* does not control expression of miR-29 and miR-130 (Figure 7). Instead, the miRNA profile of adult thymic CD8+ T cells is similar to that of neonates. In mice, the fetal thymus is colonized by at least two different layers of HSCs. The first, which is derived from the liver, colonizes the thymus around midgestation (Jotereau *et al.* 1987) and gives rise to neonatal and newborn CD8+ T cells. The second layer of hematopoietic stem cells originates from the bone marrow, and these cells seed the thymus just before birth, eventually replacing the first-layer cells and producing adult CD8+ T cells (Foss *et al.* 2001). Our data suggest that the alternative HSC origins contribute, to a degree, to differences in miRNAs expressed in neonates and adults, in particular contributing to differences observed for miR-130. By virtue of age, all neonatal and newborn CD8+ T cells have recently exited the thymus. In adults, by contrast, such recent thymic emigrants make up only ~20% of the mature CD8+ T population, and they are known to preferentially differentiate as SLECs rather than as MPECs (Makaroff *et al.* 2009; Fink 2013). Our data identify the maturity of CD8+ T cells as the major factor determining the miRNA profile, fully explaining differential levels of miR-29 and contributing to control of miR-130. To further understand the contribution of these models, it would be informative to profile miRNAs found in adult recent thymic emigrants.

Considering the large differences in naive miRNA profiles, it is interesting to consider whether miRNAs could serve as biomarkers to predict vaccine success or infection outcomes in neonates and infants. For example, because miR-29 is enriched in adult naive cells whereas miR-130 is enriched in neonatal naive cells, the ratio of miR-29 to miR-130 in naive CD8+ T cells could provide important information regarding the proportion of adult- and young-derived CD8+ T cells, which, in turn, could be used to predict if the starting population of CD8+ T cells can differentiate into long-lived memory cells. This information could be particularly useful in the clinical setting, where there appears to be extensive heterogeneity in the response to infections and vaccines during early life (Green *et al.* 1994; Hsu *et al.* 1996; Poland 1998; Nair *et al.* 2007; Gaucher *et al.* 2008; Poland *et al.* 2011).

Acknowledgments

We acknowledge the use of tissues procured by the National Disease Research Interchange with support from National Institutes of Health (NIH) grant 2 U42 OD011158. Sequencing was performed at the Cornell Biotechnology Resource Center Genomics Facility with support from NIH grant 1S10OD010693 and Cornell University. This work was supported by NIH grants R01AI105265 and R01AI110613 (to B.D.R.); grants R01GM105668 and Core B of P50HD076210 (to A.G.); the Cornell Center for Vertebrate Genomics (B.D.R. and A.G.); and National Science Foundation grant DGE-1144153 (to E.M.W.). Cytometry core is supported in part by the Empire State Stem Cell Fund, the New York State Department of Health (NYS-DOH), contract #C026718. Opinions expressed are solely the authors; they do not necessarily reflect the view of Empire State Stem Cell Board, the NYS-DOH, or New York State.

Literature Cited

Adkins, B., T. Williamson, P. Guevara, and Y. Bu, 2003 Murine neonatal lymphocytes show rapid early cell cycle entry and cell division. J. Immunol. 170: 4548–4556.

Adkins, B., C. Leclerc, and S. Marshall-Clarke, 2004 Neonatal adaptive immunity comes of age. Nat. Rev. Immunol. 4: 553–564.

Almanza, G., A. Fernandez, S. Volinia, X. Cortez-Gonzalez, C. M. Croce *et al.*, 2010 Selected microRNAs define cell fate determination of murine central memory CD8 T cells. PLoS One 5: e11243.

Banerjee, A., S. M. Gordon, A. M. Intlekofer, M. A. Paley, E. C. Mooney *et al.*, 2010 Cutting edge: the transcription factor eomesodermin enables CD8+ T cells to compete for the memory cell niche. J. Immunol. 185: 4988–4992.

Bartel, D. P., 2009 MicroRNAs: target recognition and regulatory functions. Cell 136: 215–233.
Berzins, S. P., R. L. Boyd, and J. F. P. Miller, 1998 The role of the thymus and tecent thymic migrants in the maintenance of the adult peripheral lymphocyte pool. J. Exp. Med. 187: 1839–1848.
Butz, E. A., and M. J. Bevan, 1998 Massive expansion of antigen-specific CD8+ T cells during an acute virus infection. Immunity 8: 167–175.
Campion, A. L., C. Bourgeois, F. Lambolez, B. Martin, S. Léaument *et al.*, 2002 Naive T cells proliferate strongly in neonatal mice in response to self-peptide/self-MHC complexes. Proc. Natl. Acad. Sci. USA 99: 4538–4543.
Castellino, F., and R. N. Germain, 2007 Chemokine-guided CD4+ T cell help enhances generation of IL-6RαhighIL-7Rαhigh pre-memory CD8+ T cells. J. Immunol. 178: 778–787.
Cruz-Guilloty, F., M. E. Pipkin, I. M. Djuretic, D. Levanon, J. Lotem *et al.*, 2009 Runx3 and T-box proteins cooperate to establish the transcriptional program of effector CTLs. J. Exp. Med. 206: 51–59.
D'haeseleer P., 2005 How does gene expression clustering work? Nat. Biotechnol. 23: 1499–1501.
Dooley, J., M. A. Linterman, and A. Liston, 2013 MicroRNA regulation of T-cell development. Immunol. Rev. 253: 53–64.
Ebert, M. S., and P. A. Sharp, 2012 Roles for microRNAs in conferring robustness to biological processes. Cell 149: 515–524.
Edgar, R., M. Domrachev, and A. E. Lash, 2002 Gene Expression Omnibus: NCBI gene expression and hybridization array data repository. Nucleic Acids Res. 30: 207–210.
Eichhorn, S. W., H. Guo, S. E. McGeary, R. A. Rodriguez-Mias, C. Shin *et al.*, 2014 mRNA destabilization is the dominant effect of mammalian microRNAs by the time substantial repression ensues. Mol. Cell 56: 104–115.
Fabian, M. R., N. Sonenberg, and W. Filipowicz, 2010 Regulation of mRNA translation and stability by microRNAs. Annu. Rev. Biochem. 79: 351–379.
Fink, P. J., 2013 The biology of recent thymic emigrants. Annu. Rev. Immunol. 31: 31–50.
Foss, D. L., E. Donskoy, and I. Goldschneider, 2001 The importation of hematogenous precursors by the thymus is a gated phenomenon in normal adult mice. J. Exp. Med. 193: 365–374.
Friedländer, M. R., S. D. Mackowiak, N. Li, W. Chen, and N. Rajewsky, 2012 miRDeep2 accurately identifies known and hundreds of novel microRNA genes in seven animal clades. Nucleic Acids Res. 40: 37–52.
Friedman, R. C., K. K.-H. Farh, C. B. Burge, and D. P. Bartel, 2009 Most mammalian mRNAs are conserved targets of microRNAs. Genome Res. 19: 92–105.
Garcia, D. M., D. Baek, C. Shin, G. W. Bell, A. Grimson *et al.*, 2011 Weak seed-pairing stability and high target-site abundance decrease the proficiency of lsy-6 and other microRNAs. Nat. Struct. Mol. Biol. 18: 1139–1146.
Gaucher, D., R. Therrien, N. Kettaf, B. R. Angermann, G. Boucher *et al.*, 2008 Yellow fever vaccine induces integrated multilineage and polyfunctional immune responses. J. Exp. Med. 205: 3119–3131.
Gerlach, C., J. W. J. van Heijst, E. Swart, D. Sie, N. Armstrong *et al.*, 2010 One naive T cell, multiple fates in CD8+ T cell differentiation. J. Exp. Med. 207: 1235–1246.
Gracias, D. T., E. Stelekati, J. L. Hope, A. C. Boesteanu, T. A. Doering *et al.*, 2013 The microRNA miR-155 controls CD8(+) T cell responses by regulating interferon signaling. Nat. Immunol. 14: 593–602.
Green, M. S., T. Shohat, Y. Lerman, D. Cohen, R. Slepon *et al.*, 1994 Sex differences in the humoral antibody response to live measles vaccine in young adults. Int. J. Epidemiol. 23: 1078–1081.
Guo, H., N. T. Ingolia, J. S. Weissman, and D. P. Bartel, 2010 Mammalian microRNAs predominantly act to decrease target mRNA levels. Nature 466: 835–840.
Hale, J. S., T. E. Boursalian, G. L. Turk, and P. J. Fink, 2006 Thymic output in aged mice. Proc. Natl. Acad. Sci. USA 103: 8447–8452.
Harty, J. T., A. R. Tvinnereim, and D. W. White, 2000 CD8+ T cell effector mechanisms in resistance to infection. Annu. Rev. Immunol. 18: 275–308.
Hsu, L.-C., S.-R. Lin, H.-M. Hsu, W.-H. Chao, J.-T. Hsieh *et al.*, 1996 Ethnic differences in immune responses to hepatitis B vaccine. Am. J. Epidemiol. 143: 718–724.
Intlekofer, A. M., N. Takemoto, E. J. Wherry, S. A. Longworth, J. T. Northrup *et al.*, 2005 Effector and memory CD8+ T cell fate coupled by T-bet and eomesodermin. Nat. Immunol. 6: 1236–1244.
Joshi, N. S., and S. M. Kaech, 2008 Effector CD8 T cell development: a balancing act between memory cell potential and terminal differentiation. J. Immunol. 180: 1309–1315.
Joshi, N. S., W. Cui, A. Chandele, H. K. Lee, D. R. Urso *et al.*, 2007 Inflammation directs memory precursor and short-lived effector CD8+ T cell fates via the graded expression of T-bet transcription factor. Immunity 27: 281–295.
Jotereau, F., F. Heuze, V. Salomon-Vie, and H. Gascan, 1987 Cell kinetics in the fetal mouse thymus: precursor cell input, proliferation, and emigration. J. Immunol. 138: 1026–1030.
Jung, Y. W., R. L. Rutishauser, N. S. Joshi, A. M. Haberman, and S. M. Kaech, 2010 Differential localization of effector and memory CD8 T cell subsets in lymphoid organs during acute viral infection. J. Immunol. 185: 5315–5325.
Kaech, S. M., and W. Cui, 2012 Transcriptional control of effector and memory CD8+ T cell differentiation. Nat. Rev. Immunol. 12: 749–761.
Kaech, S. M., S. Hemby, E. Kersh, and R. Ahmed, 2002 Molecular and functional profiling of memory CD8 T cell differentiation. Cell 111: 837–851.
Khan, A. A., L. A. Penny, Y. Yuzefpolskiy, S. Sarkar, and V. Kalia, 2013 MicroRNA-17∼92 regulates effector and memory CD8 T-cell fates by modulating proliferation in response to infections. Blood 121: 4473–4483.
Kim, V. N., and J.-W. Nam, 2006 Genomics of microRNA. Trends Genet. 22: 165–173.
Kroesen, B.-J., N. Teteloshvili, K. Smigielska-Czepiel, E. Brouwer, A. M. H. Boots *et al.*, 2015 Immuno-miRs: critical regulators of T-cell development, function and ageing. Immunology 144: 1–10.
Lewis, B. P., I. Shih, M. W. Jones-Rhoades, D. P. Bartel, and C. B. Burge, 2003 Prediction of mammalian microRNA targets. Cell 115: 787–798.
Li, G., M. Yu, W.-W. Lee, M. Tsang, E. Krishnan *et al.*, 2012 Decline in miR-181a expression with age impairs T cell receptor sensitivity by increasing DUSP6 activity. Nat. Med. 18: 1518–1524.
Liang, Y., H.-F. Pan, and D.-Q. Ye, 2015 microRNAs function in CD8+T cell biology. J. Leukoc. Biol. 97: 487–497.
Lianoglou, S., V. Garg, J. L. Yang, C. S. Leslie, and C. Mayr, 2013 Ubiquitously transcribed genes use alternative polyadenylation to achieve tissue-specific expression. Genes Dev. 27: 2380–2396.
Ma, F., S. Xu, X. Liu, Q. Zhang, X. Xu *et al.*, 2011 The microRNA miR-29 controls innate and adaptive immune responses to intracellular bacterial infection by targeting interferon-γ. Nat. Immunol. 12: 861–869.
Makaroff, L. E., D. W. Hendricks, R. E. Niec, and P. J. Fink, 2009 Postthymic maturation influences the CD8 T cell response to antigen. Proc. Natl. Acad. Sci. USA 106: 4799–4804.
Mayr, C., and D. P. Bartel, 2009 Widespread shortening of 3′UTRs by alternative cleavage and polyadenylation activates oncogenes in cancer cells. Cell 138: 673–684.
Mukherji, S., M. S. Ebert, G. X. Y. Zheng, J. S. Tsang, P. A. Sharp *et al.*, 2011 MicroRNAs can generate thresholds in target gene expression. Nat. Genet. 43: 854–859.

Muljo, S. A., K. M. Ansel, C. Kanellopoulou, D. M. Livingston, A. Rao *et al.*, 2005 Aberrant T cell differentiation in the absence of Dicer. J. Exp. Med. 202: 261–269.

Nair, N., H. Gans, L. Lew-Yasukawa, A. C. Long-Wagar, A. Arvin *et al.*, 2007 Age-dependent differences in IgG isotype and avidity induced by measles vaccine received during the first year of life. J. Infect. Dis. 196: 1339–1345.

Nam, J.-W., O. S. Rissland, D. Koppstein, C. Abreu-Goodger, C. H. Jan *et al.*, 2014 Global analyses of the effect of different cellular contexts on microRNA targeting. Mol. Cell 53: 1031–1043.

Neilson, J. R., G. X. Y. Zheng, C. B. Burge, and P. A. Sharp, 2007 Dynamic regulation of miRNA expression in ordered stages of cellular development. Genes Dev. 21: 578–589.

Opiela, S. J., T. Koru-Sengul, and B. Adkins, 2009 Murine neonatal recent thymic emigrants are phenotypically and functionally distinct from adult recent thymic emigrants. Blood 113: 5635–5643.

Palin, A. C., V. Ramachandran, S. Acharya, and D. B. Lewis, 2013 Human neonatal naive CD4+ T cells have enhanced activation-dependent signaling regulated by the microRNA miR-181a. J. Immunol. 190: 2682–2691.

Penninger, J. M., C. Sirard, H. W. Mittrücker, A. Chidgey, I. Kozieradzki *et al.*, 1997 The interferon regulatory transcription factor IRF-1 controls positive and negative selection of CD8+ thymocytes. Immunity 7: 243–254.

Pipkin, M. E., J. A. Sacks, F. Cruz-Guilloty, M. G. Lichtenheld, M. J. Bevan *et al.*, 2010 Interleukin-2 and inflammation induce distinct transcriptional programs that promote the differentiation of effector cytolytic T cells. Immunity 32: 79–90.

Poland, G. A., 1998 Variability in immune response to pathogens: using measles vaccine to probe immunogenetic determinants of response. Am. J. Hum. Genet. 62: 215–220.

Poland, G. A., R. B. Kennedy, and I. G. Ovsyannikova, 2011 Vaccinomics and personalized vaccinology: Is science leading us toward a new path of directed vaccine development and discovery? PLoS Pathog. 7: e1002344.

Rao, R. R., Q. Li, K. Odunsi, and P. A. Shrikant, 2010 The mTOR Kinase determines effector *vs.* memory CD8+ T cell fate by regulating the expression of transcription factors T-bet and eomesodermin. Immunity 32: 67–78.

Rao, R. R., Q. Li, M. R. G. Bupp, and P. A. Shrikant, 2012 Transcription factor Foxo1 represses T-bet-mediated effector functions and promotes memory CD8+ T cell differentiation. Immunity 36: 374–387.

Reynolds, A. P., G. Richards, B. de la Iglesia, and V. J. Rayward-Smith, 2006 Clustering rules: a comparison of partioning and hierarchical clustering algorithms. J. Math. Model. Algor. 5: 475–504.

Robinson, M. D., D. J. McCarthy, and G. K. Smyth, 2010 edgeR: a Bioconductor package for differential expression analysis of digital gene expression data. Bioinformatics 26: 139–140.

Rudd, B. D., V. Venturi, M. P. Davenport, and J. Nikolich-Zugich, 2011 Evolution of the antigen-specific CD8+ TCR repertoire across the life span: evidence for clonal homogenization of the old TCR repertoire. J. Immunol. 186: 2056–2064.

Rudd, B. D., V. Venturi, N. L. Smith, K. Nzingha, E. L. Goldberg *et al.*, 2013 Acute neonatal infections "lock-in" a suboptimal CD8+ T cell repertoire with impaired recall responses. PLoS Pathog. 9: e1003572.

Sandberg, R., J. R. Neilson, A. Sarma, P. A. Sharp, and C. B. Burge, 2008 Proliferating cells express mRNAs with shortened 3′ untranslated regions and fewer microRNA target sites. Science 320: 1643–1647.

Sarkar, S., V. Kalia, W. N. Haining, B. T. Konieczny, S. Subramaniam *et al.*, 2008 Functional and genomic profiling of effector CD8 T cell subsets with distinct memory fates. J. Exp. Med. 205: 625–640.

Sayed, D., and M. Abdellatif, 2011 MicroRNAs in development and disease. Physiol. Rev. 91: 827–887.

Schwarz, B. A., and A. Bhandoola, 2006 Trafficking from the bone marrow to the thymus: a prerequisite for thymopoiesis. Immunol. Rev. 209: 47–57.

Shiow, L. R., D. B. Rosen, N. Brdičková, Y. Xu, J. An *et al.*, 2006 CD69 acts downstream of interferon-α/β to inhibit S1P1 and lymphocyte egress from lymphoid organs. Nature 440: 540–544.

Smith, N. L., E. Wissink, J. Wang, J. F. Pinello, M. P. Davenport *et al.*, 2014 Rapid proliferation and differentiation impairs the development of memory CD8+ T cells in early life. J. Immunol. 193: 177–184.

Starr, T. K., S. C. Jameson, and K. A. Hogquist, 2003 Positive and negative selection of T cells. Annu. Rev. Immunol. 21: 139–176.

Stefani, G., and F. J. Slack, 2008 Small non-coding RNAs in animal development. Nat. Rev. Mol. Cell Biol. 9: 219–230.

Subramanian, A., P. Tamayo, V. K. Mootha, S. Mukherjee, B. L. Ebert *et al.*, 2005 Gene set enrichment analysis: a knowledge-based approach for interpreting genome-wide expression profiles. Proc. Natl. Acad. Sci. USA 102: 15545–15550.

Takemoto, N., A. M. Intlekofer, J. T. Northrup, E. J. Wherry, and S. L. Reiner, 2006 Cutting edge: IL-12 inversely regulates T-bet and eomesodermin expression during pathogen-induced CD8+ T cell differentiation. J. Immunol. 177: 7515–7519.

Trapnell, C., L. Pachter, and S. L. Salzberg, 2009 TopHat: discovering splice junctions with RNA-Seq. Bioinformatics 25: 1105–1111.

Trapnell, C., D. G. Hendrickson, M. Sauvageau, L. Goff, J. L. Rinn *et al.*, 2013 Differential analysis of gene regulation at transcript resolution with RNA-seq. Nat. Biotechnol. 31: 46–53.

Trifari, S., M. E. Pipkin, H. S. Bandukwala, T. Äijö, J. Bassein *et al.*, 2013 MicroRNA-directed program of cytotoxic CD8+ T-cell differentiation. Proc. Natl. Acad. Sci. USA 110: 18608–18613.

Tsai, C.-Y., S. R. Allie, W. Zhang, and E. J. Usherwood, 2013 MicroRNA miR-155 affects antiviral effector and effector memory CD8 T cell differentiation. J. Virol. 87: 2348–2351.

Weinreich, M. A., and K. A. Hogquist, 2008 Thymic emigration: when and how T cells leave home. J. Immunol. 181: 2265–2270.

Williams, M. A., and M. J. Bevan, 2007 Effector and memory CTL differentiation. Annu. Rev. Immunol. 25: 171–192.

Wu, H., J. R. Neilson, P. Kumar, M. Manocha, P. Shankar *et al.*, 2007 miRNA profiling of naïve, effector and memory CD8 T cells. PLoS One 2: e1020.

Wu, T., A. Wieland, K. Araki, C. W. Davis, L. Ye *et al.*, 2012 Temporal expression of microRNA cluster miR-17–92 regulates effector and memory CD8+ T-cell differentiation. Proc. Natl. Acad. Sci. USA 109: 9965–9970.

Xiao, C., and K. Rajewsky, 2009 MicroRNA control in the immune system: basic principles. Cell 136: 26–36.

Yang, C. Y., J. A. Best, J. Knell, E. Yang, A. D. Sheridan *et al.*, 2011 The transcriptional regulators Id2 and Id3 control the formation of distinct memory CD8+ T cell subsets. Nat. Immunol. 12: 1221–1229.

Yang, L., M. P. Boldin, Y. Yu, C. S. Liu, C.-K. Ea *et al.*, 2012 miR-146a controls the resolution of T cell responses in mice. J. Exp. Med. 209: 1655–1670.

Zhang, N., and M. J. Bevan, 2010 Dicer controls CD8+ T-cell activation, migration, and survival. Proc. Natl. Acad. Sci. USA 107: 21629–21634.

Communicating editor: A. Gasch

GENETICS

Supporting Information
www.genetics.org/lookup/suppl/doi:10.1534/genetics.115.179176/-/DC1

MicroRNAs and Their Targets Are Differentially Regulated in Adult and Neonatal Mouse CD8+ T Cells

Erin M. Wissink, Norah L. Smith, Roman Spektor, Brian D. Rudd, and Andrew Grimson

DOI: 10.1534/genetics.115.179176

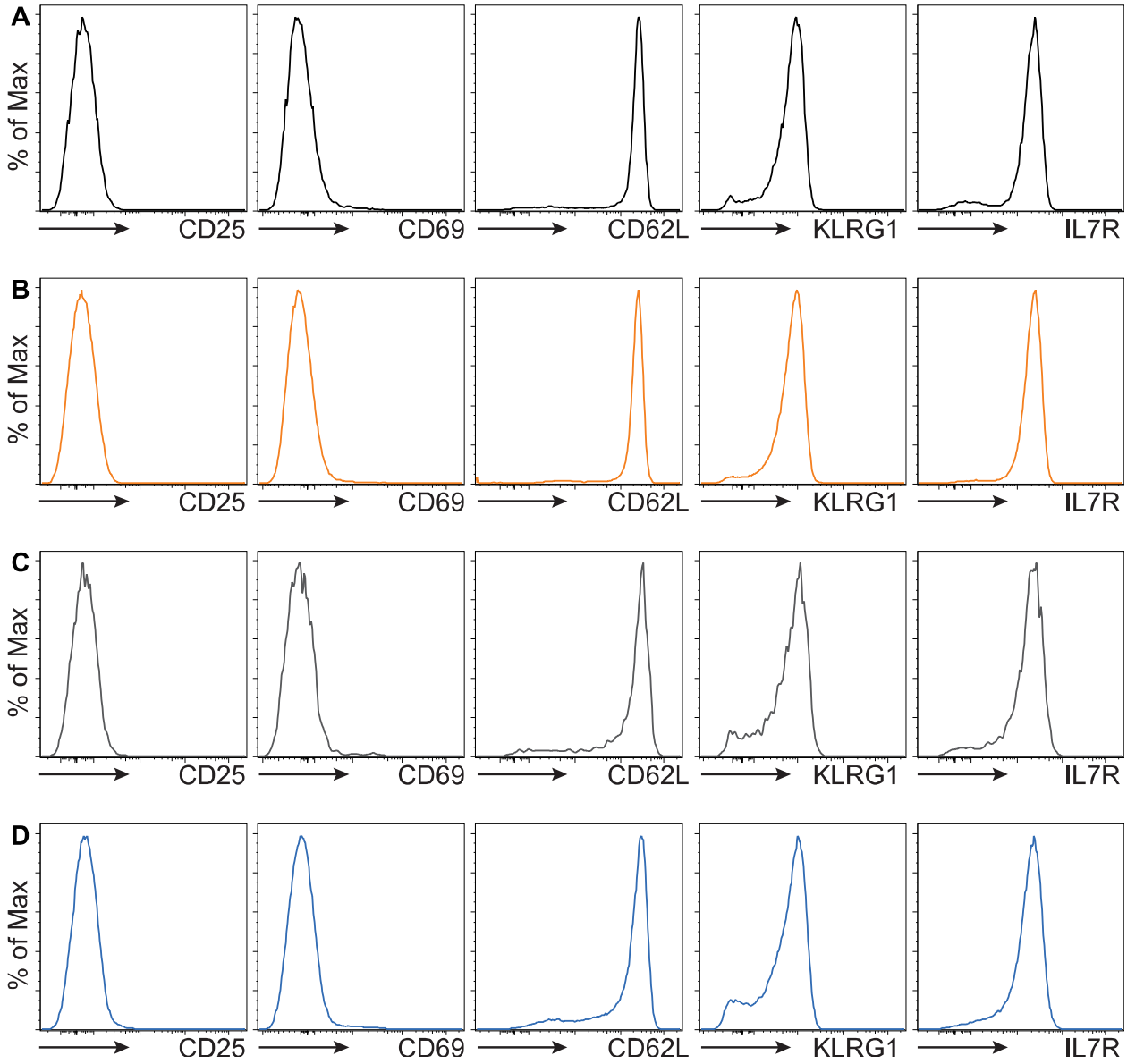

Figure S1 Adult and neonatal CD8+ T cells have equivalent phenotypes before and after selection. Representative histograms show expression of IL2RA/CD25 (associated with activation), CD69 (associated with activation), SELL/CD62L (marker of lymph homing), KLRG1 (marker of SLECs), and IL7R (marker of MPECs) in naive CD8+ cells from (A) adults pre-selection, (B) adults post-selection, (C) neonates pre-selection, and (D) neonates post-selection.

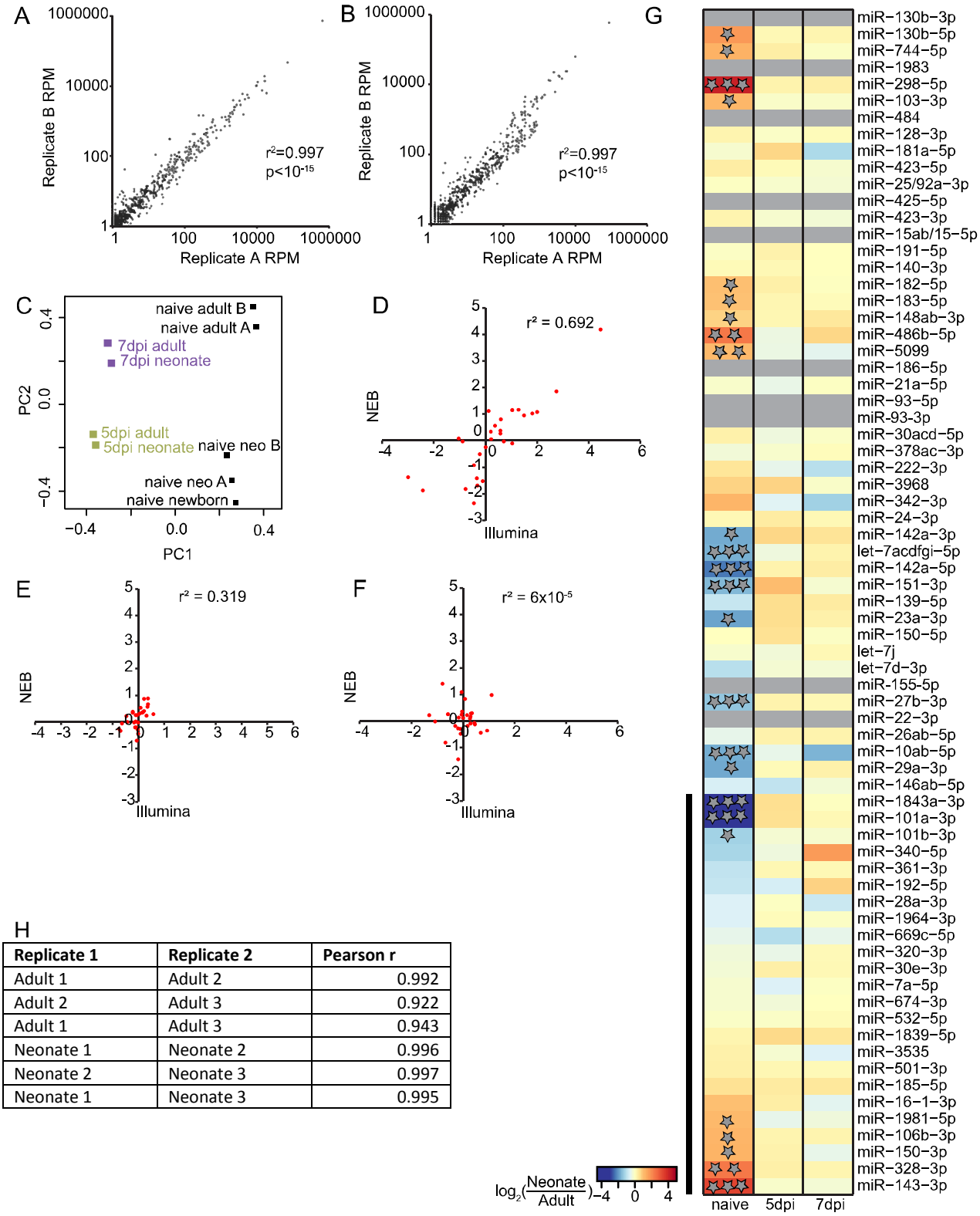

H

Replicate 1	Replicate 2	Pearson r
Adult 1	Adult 2	0.992
Adult 2	Adult 3	0.922
Adult 1	Adult 3	0.943
Neonate 1	Neonate 2	0.996
Neonate 2	Neonate 3	0.997
Neonate 1	Neonate 3	0.995

Figure S2 Differences in miRNA expression are conserved in biological replicates and robust to alterative sequencing protocols. (A and B) Correlation of miRNA expression between two mouse naive CD8+ T cell biological replicates. The reads per million (RPM) of all miRNAs with at least one read are shown for adult (A) and neonatal (B) samples. (C) Principal component analysis on all replicate samples for miRNA sequencing. (D-F) Correlation of miRNA neonatal:adult fold-change values for miRNA sequencing libraries derived from Illumina TruSeq and NEBNext protocols in naive (D), 5-dpi (E), and 7-dpi (F) cells. (G) Heatmap of neonatal:adult fold-change for miRNAs sequenced using the NEBNext protocol. miRNAs marked with a black bar are miRNAs that were captured by the TruSeq protocol, and miRNAs in gray are ones that were not captured by the NEBNext protocol. Differential expression was determined by edgeR. *=$p<0.05$, **=$p<0.005$, ***=$p<0.0005$. (H) Pearson correlation coefficients for all pairwise combinations of human biological replicates, based on miRNAs with at least one read in one of the samples.

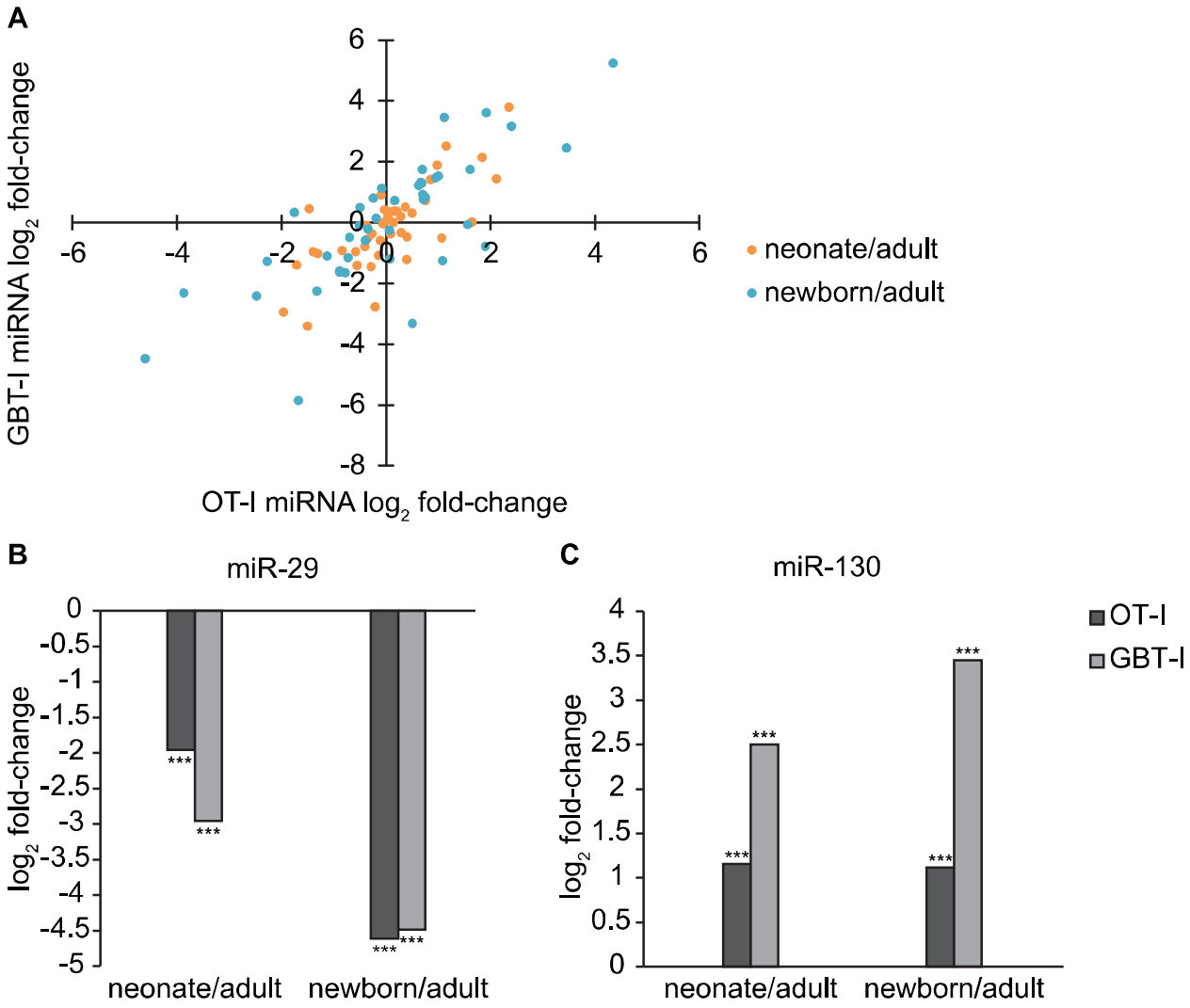

Figure S3 CD8+ T cells from two transgenic TCR mouse strains have similar age-dependent miRNA expression differences. (A) Correlation of fold-changes in neonatal:adult (Pearson r=0.753) and newborn:adult (Pearson r=0.765) miRNA expression between gBT-I and OT-I naive CD8+ T cell biological replicates. Fold-change values were calculated with edgeR; each sample corresponded to two biological replicates, except the gBT-I newborn, which had one. (B) Fold-change in expression of miR-29a between adults and neonates, or adults and newborns, for OT-I and gBT-I naive CD8+ T cells. Differential expression was determined by edgeR; ***=p<0.0005. (C) Fold-change in expression of miR-130b between adults and neonates, or adults and newborns, for OT-I and gBT-I naive CD8+ T cells. Differential expression was determined by edgeR; ***=p<0.0005.

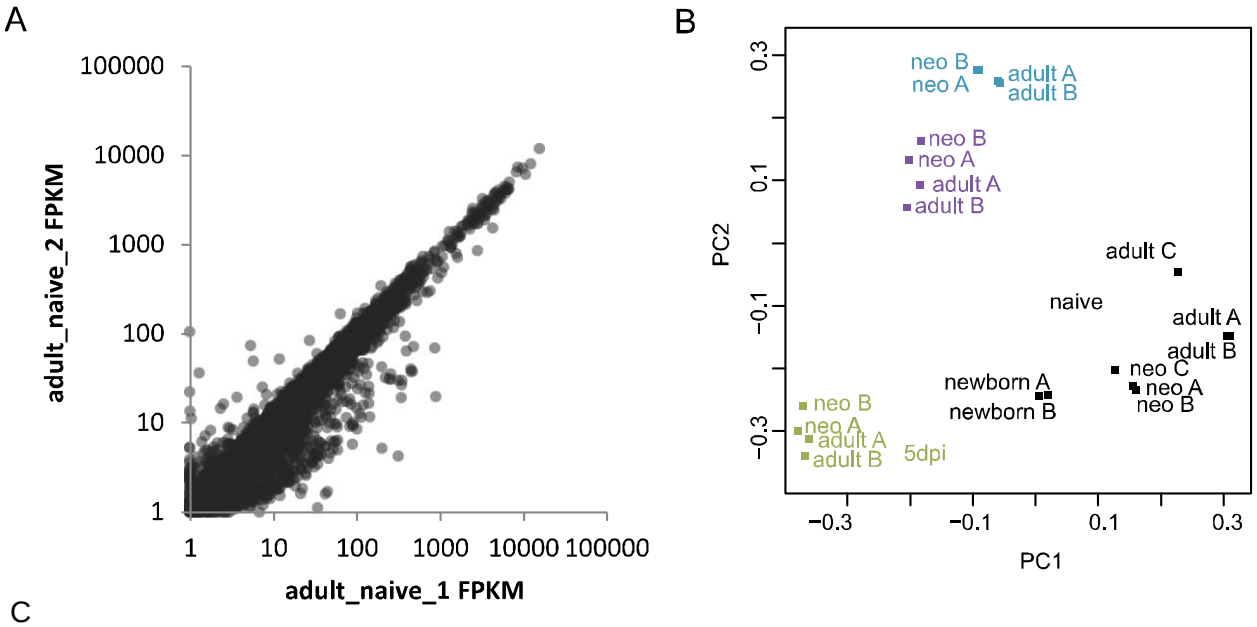

C

Replicate 1	Replicate 2	Pearson R	Pearson p value	Spearman ρ	Spearman p value
adult_naive_0	adult_naive_1	0.99891	$<10^{-15}$	0.99573	$<10^{-15}$
adult_naive_0	adult_naive_2	0.98925	$<10^{-15}$	0.96091	$<10^{-15}$
adult_naive_1	adult_naive_2	0.98826	$<10^{-15}$	0.96041	$<10^{-15}$
adult_5dpi_0	adult_5dpi_1	0.99823	$<10^{-15}$	0.99763	$<10^{-15}$
adult_7dpi_0	adult_7dpi_1	0.99824	$<10^{-15}$	0.99651	$<10^{-15}$
adult_15dpi_0	adult_15dpi_1	0.99954	$<10^{-15}$	0.99823	$<10^{-15}$
neonate_naive_0	neonate_naive_1	0.99769	$<10^{-15}$	0.99009	$<10^{-15}$
neonate_naive_0	neonate_naive_2	0.99408	$<10^{-15}$	0.98841	$<10^{-15}$
neonate_naive_1	neonate_naive_2	0.99207	$<10^{-15}$	0.98722	$<10^{-15}$
neonate_5dpi_0	neonate_5dpi_1	0.99515	$<10^{-15}$	0.9964	$<10^{-15}$
neonate_7dpi_0	neonate_7dpi_1	0.99434	$<10^{-15}$	0.99671	$<10^{-15}$
neonate_15dpi_0	neonate_15dpi_1	0.99891	$<10^{-15}$	0.99785	$<10^{-15}$
newborn_naive_0	newborn_naive_1	0.99870	$<10^{-15}$	0.99558	$<10^{-15}$

Figure S4 mRNA profiles determined by high-throughput sequencing compared between biological replicate samples. (A) Genes that were well-expressed (FPKM>1 in at least one sample) were used; expression values (FPKM) for well-expressed genes (11,360) are shown for two biological replicates. (B) Principal component analysis was performed on all replicate samples for well-expressed genes. (C) Pearson and Spearman correlation coefficients for all pairs of biological replicates that underwent mRNA sequencing.

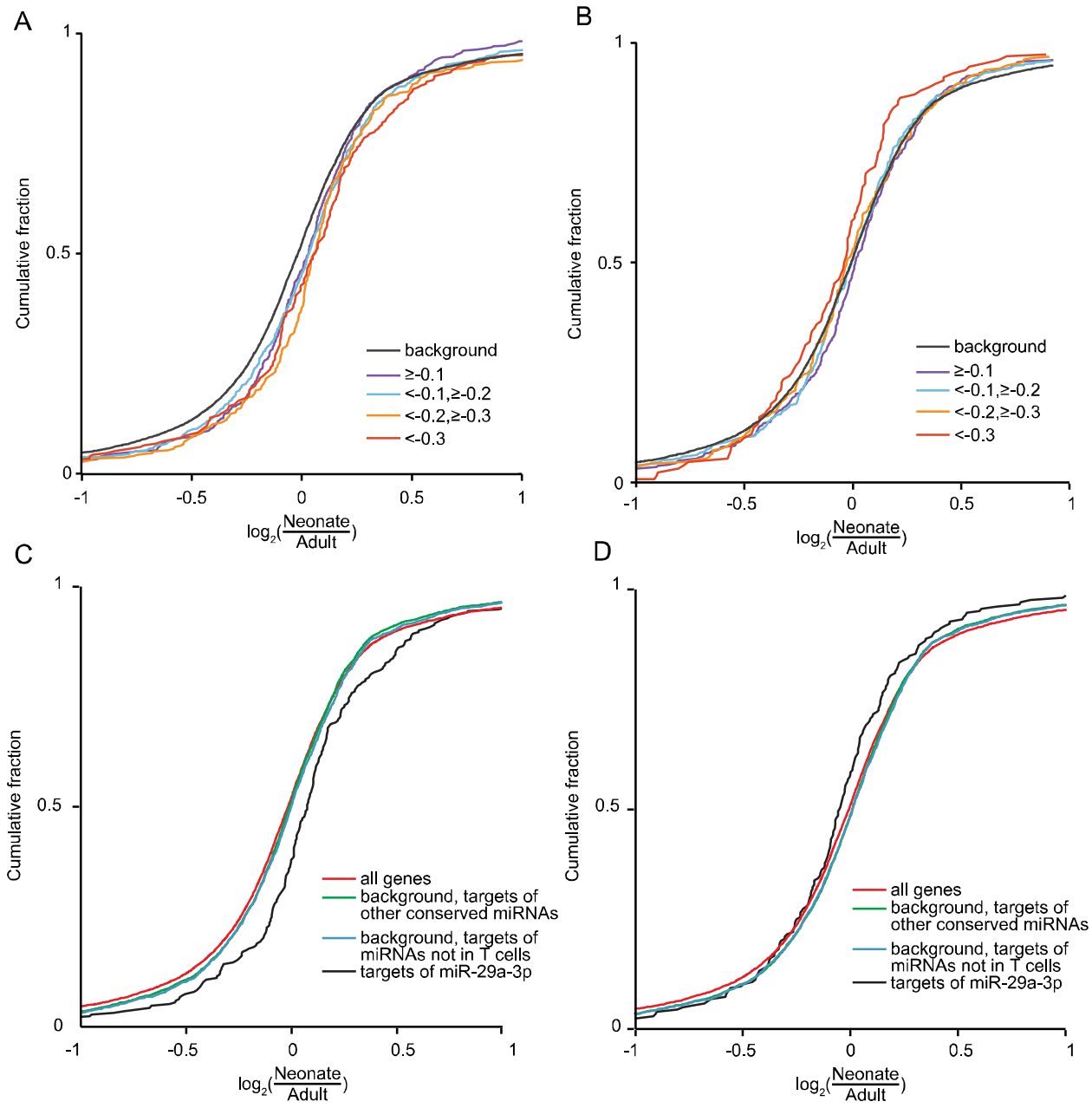

Figure S5 miRNA targeting analysis. (A and B) Targets of miR-29a-3p (A) and miR-130b-3p (B) were binned by context score, regardless of conservation status, to confirm that stronger targets were more repressed by their cognate miRNA than were weaker targets. The background set used was all well-expressed genes, excluding targets for the miRNA being tested. For miR-29a-3p, all context score bins are significantly different from background (context ≥-0.1, $p<0.05$; context <-0.1, ≥-0.2, $p<0.005$; context <-0.2, ≥-0.3, $p<10^{-6}$; context <-0.3, $p<0.05$). For miR-130b-3p, targets with context scores <-0.3 were significantly different from background ($p<0.05$). (C and D) MicroRNA targeting signatures are robust to alternative background gene sets. We tested background sets consisting of all well-expressed genes (red), well-expressed genes that are strong targets of broadly conserved miRNAs (defined in Friedman *et al.* 2009, green), and well-expressed genes that are targets of broadly conserved miRNAs excluding those well-expressed in CD8+ T cells. Compared to all background sets, strong miR-29a-3p targets (C, gray) have significantly different expression ($p<0.0005$). Similarly, strong miR-130b-3p targets (D, gray) have significantly different expression ($p<0.05$) when compared to all different background sets tested.

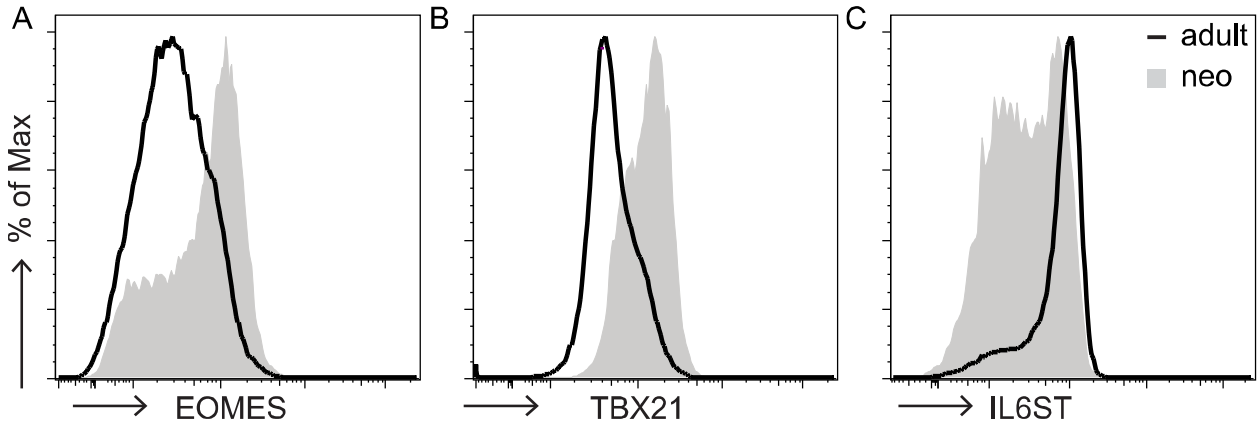

Figure S6 Representative flow cytometry plots. Protein expression in naive adult and neonatal CD8+ T cells of EOMES (A), TBX21 (B), and IL6ST (C) were quantified by flow cytometry.

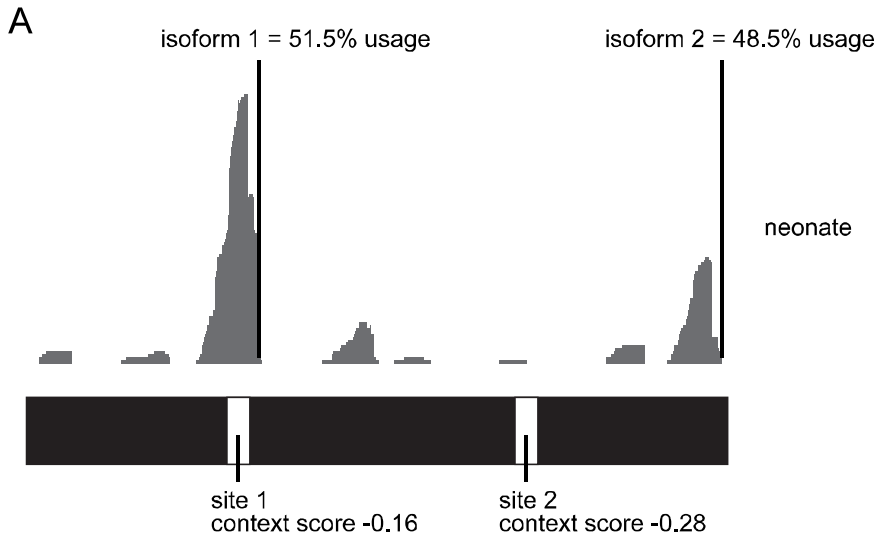

Actual score=(isoform 1 usage x site 1 score) + (isoform 2 usage x site 1 score) + (isoform 2 usage x site 2 score)
Acutal score=(0.515 x -0.16) + (0.485 x -0.16) + (0.485 x -0.28) = -0.29429
Expected score=-0.16-0.28=-0.44

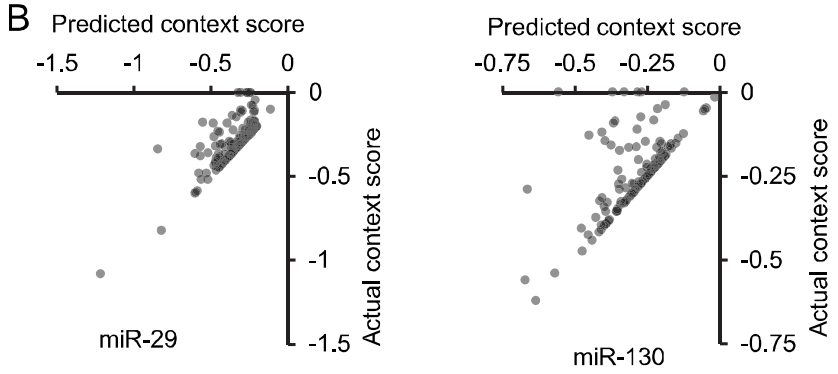

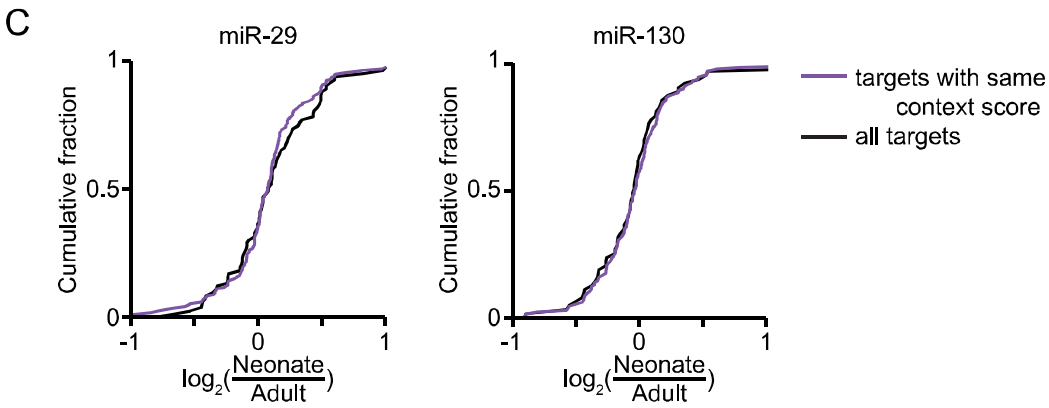

Figure S7 Context scores for isoforms of miRNA targets expressed in CD8+ T cells. (A) Example of calculation of actual context scores using experimentally verified 3'UTR isoforms. For each target, we found expressed isoforms (each isoform consisting of ≥20% of the reads for that gene), then found the context scores for the individual miRNA target sites in all expressed isoforms. We calculated an average context scores of the target sites, weighting them by the usage of that site, as determined by 3'-Seq. *Eomes* has two isoforms and two target sites. One target site is found in both isoforms, whereas the second is found only in the longer isoform. Their scores are weighted based on site usage (51.5% usage for site 1 and 48.5% usage for site 2 in neonates). (B) For each strong predicted target of miR-29a-3p (left) or miR-130b-3p (right), we calculated an actual context score, taking into account the miRNA target sites present. We then compared the average context score for adults and neonates to the expected score (Pearson r=0.789 for miR-29a-3p targets; Pearson r=0.628 for miR-130b-3p targets); high correlations indicate most, but not all, targets have very similar context scores to predicted. (C) We compared the fold-change difference in expression for all predicted targets of miR-29a-3p (left) and miR-130b-3p (right) to fold-change differences for only targets whose experimentally determined isoforms have the predicted context scores. The two groups are not significantly different according to two-sided Kolmogorov–Smirnov tests (miR-29a-3p: p=0.825; miR-130b-3p: p=0.991).

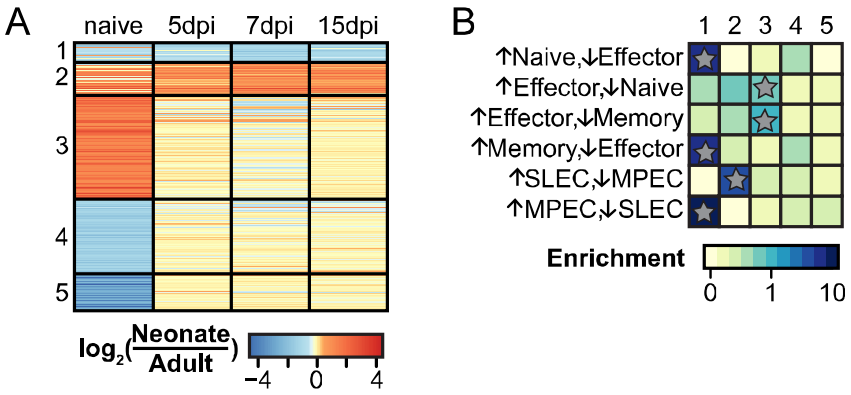

Figure S8 Clustering gene expression differences between adults and neonates. (A) Clustering of co-regulated genes in neonatal and adult CD8+ T cell transcriptomes. Fold-change differences for genes with significant differential expression between adults and neonates were calculated, and fold-differences used to cluster co-regulated groups of genes (as described in Figure 6); see also File S7. (B) Genes in each cluster were compared to genes that define naive, effector, memory cells, MPEC, or SLEC cells. Enrichment was calculated as number of genes in each cluster as compared to the number expected. Significance was determined by Fisher exact tests, *$p<10^{-4}$.

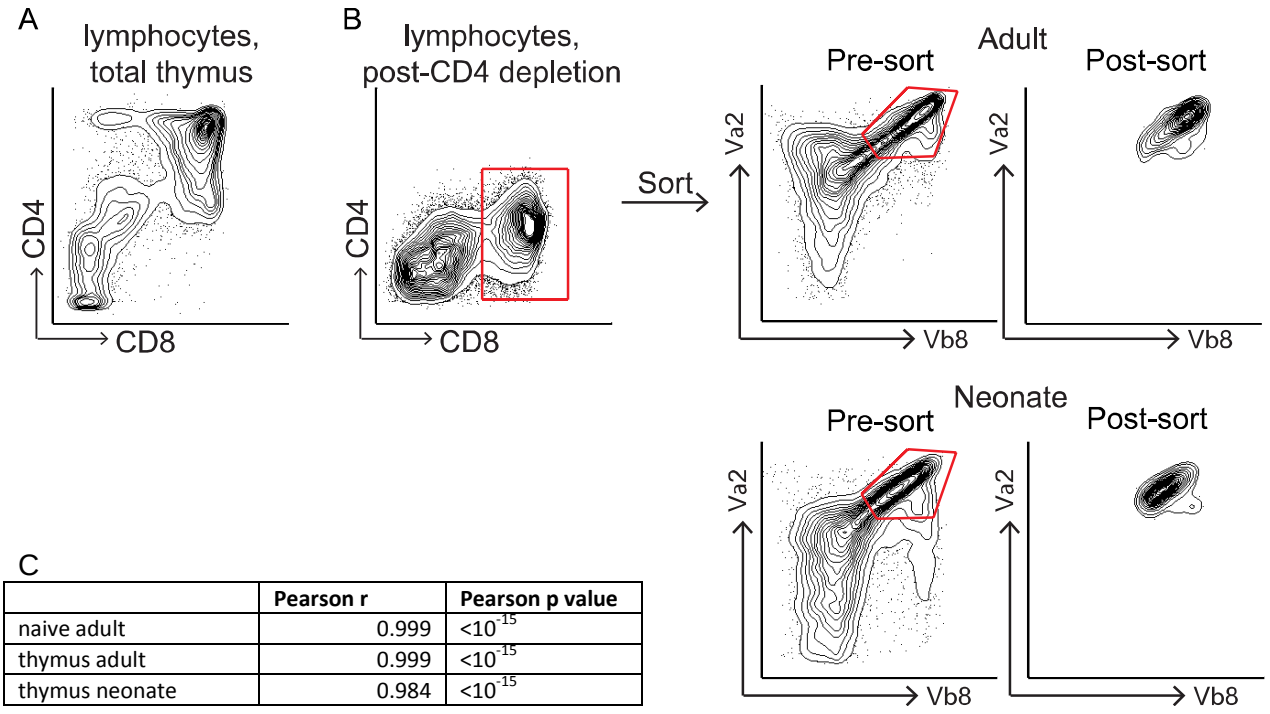

C

	Pearson r	Pearson p value
naive adult	0.999	$<10^{-15}$
thymus adult	0.999	$<10^{-15}$
thymus neonate	0.984	$<10^{-15}$

Figure S9 Thymus cells. (A) Distribution of CD4+ and CD8+ T cells in thymus. (B) Sorting strategy. Thymic cells were depleted of CD4+ cells, then Va2+ Vb8+ cells were FACS sorted to >90% purity. The sorted populations are shown in red boxes. (C) Pearson correlation coefficients for biological replicate miRNA sequencing data.

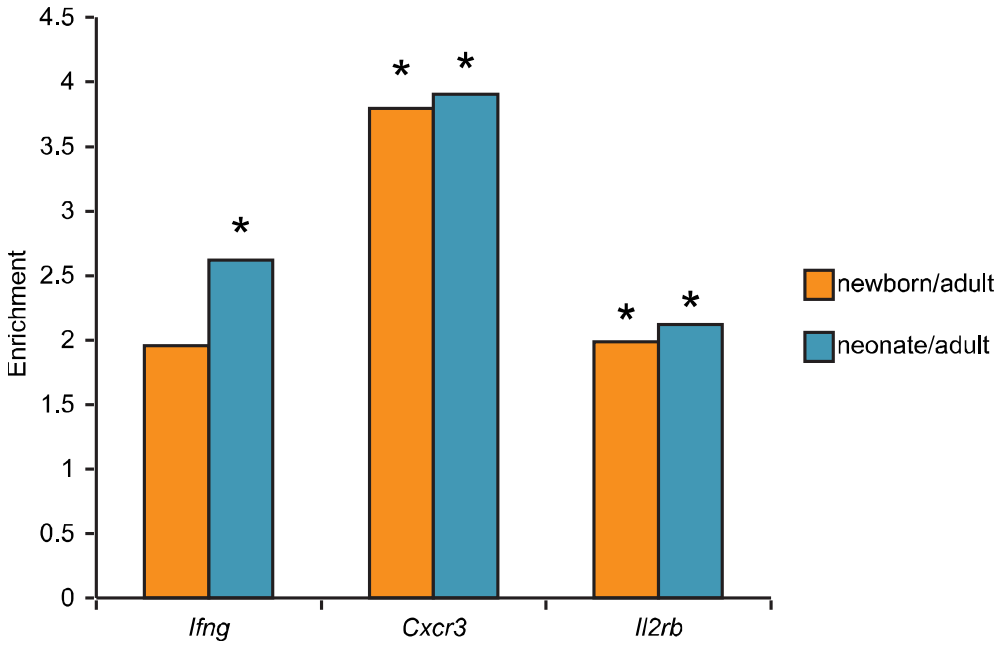

Figure S10 Expression differences for genes regulated by *Tbx21* and *Eomes*. Fold-change differences for genes were calculated between newborn/neonate and adults; *Benjamini-Hochberg corrected p<0.05.

File S1
Supporting Materials and Methods

Preparation of human samples. Whole blood samples from adults and cord blood were obtained from New York Blood Center (Long Island City, NY) and National Disease Research Interchange (Philadelphia, PA), respectively. To isolate mononuclear cells from whole blood, samples were mixed with 1-2 times their volume of PBS-EDTA. This diluted blood was layered over Ficoll-paque Plus (GE Healthcare), then centrifuged at 400g for 30 minutes at room temperature. Mononuclear cells at the interface between plasma and Ficoll were collected and washed with PBS-EDTA. To isolate CD8+ T cells from this fraction, a Naive CD8+ T Cell Isolation Kit (human) (Miltenyi) was used according to manufacturers' instructions. Following isolation, cells were placed in Trizol (Life Technologies).

Mice. gBT-I TCR transgenic mice (TCRαβ specific for SSIEFARL peptide from HSV-1 glycoprotein B498-505) were provided by Dr. Janko Nikolich-Zugich (University of Arizona, Tucson, AZ). Ly5.2 mice (8-12 wk) were purchase from The National Cancer Institute (Fredrick, MD). Rag-/- OT-I mice were purchased from Taconic (Germantown, NY) and were crossed to C57Bl/6 mice from The National Cancer Institute and F1 progeny were used.

Antibodies, Staining and Flow Cytometry. The fluorochrome labeled monoclonal antibodies anti-CD8α (53-6.7), anti-CD4 (GK1.5), anti-CD45.1 (A20), anti-CD45.2 (104), anti-CD90.1/Thy1.1 (OX-7), anti-KLRG1 (2F1), anti-CD127 (A7R34), anti-CD62L (MEL-14), anti-CD44 (clone), anti-Eomes (Dan11mag), anti-T-bet (eBio4B10), anti-CXCR3 (CXCR3-173), anti-CCR5 (HM-CCR5), anti-CCR7 (4B12) and anti-gp130 (KGP130) were purchased from Biolegend (San Diego, CA), eBioscience (San Diego, CA), Life technologies (Carlsbad, CA) or BD Biosciences (San Jose, CA).

Sorting. Splenocytes were harvested and positive magnetic selection was performed using anti-CD8 beads (Miltenyi Biotec, Auburn, CA), according to manufacturer's instructions. Following purification, cells were labeled with anti-CD4-fluorescein isothiocyanate, anti-CD8-e450, anti-Thy1.1-allophycocyanin, anti-CD45.2,-allophcyocyanin-e780 and anti-CD45.1-phycoerythrin-Cy7 for 30 min at 4°C. Labeled cells were washed twice and placed in sorting buffer (PBS, 0.5% BSA, 2 mM EDTA). We concurrently sorted for CD8+CD4-CD45.1-CD45.2+Thy1.1+ and CD8+CD4-CD45.1-CD45.2+Thy1.1- populations and achieved >95% purity. Sorting was performed on a FACS Aria (BD Biosciences).

RNA isolation. Cells were resuspended in Trizol (Life Technologies) at a concentration of 1 million cells/mL and stored at -80°C. RNA isolation was completed within a month. To do so, the samples were thawed and 200 µL of chloroform per mL Trizol was added. The tubes were shook for 15 seconds, then incubated at room temperature for ten minutes to allow for phase

separation. The tubes were centrifuged for 15 minutes at 12,000xg at 4°C. The upper aqueous phase was transferred to a fresh tube, and 1 µL glycoblue (Life Technologies) was added to help visualize the RNA pellet. To precipitate the RNA, we added 0.5 mL isopropanol per mL Trizol, then incubated at room temperature for ten minutes, then centrifuged for ten minutes at 12,000xg at 4°C. The supernatant was pipetted off, and the pellet was washed in 1 mL 75% ethanol, then centrifuged for ten minutes at 12,000xg at 4°C. The supernatant was pipetted off and the RNA pellet was allowed to air dry for ten minutes. The RNA was then resuspended in 20 µL RNase-free water (HyClone).

Small RNA-Seq analysis. We used miRDeep2 to align and quantify sequencing reads to known mouse miRNAs (Friedländer *et al.* 2012). For aligning, we inputted the raw sequencing files into the script mapper.pl (a component of miRDeep2) which trimmed the adapter sequence (TGGAATTCTCGGGTGCCAAGG for libraries generated with Illumina, AGATCGGAAGAGCACACGTCT for libraries generated with NEB), discarded reads with fewer than 18 nucleotides, aligned the reads to the genome (mm9) using Bowtie (Langmead *et al.* 2009). We used options –e, -h, -i, -j, -k, -l 18, and -m.

Genome-matching reads were matched to known mouse miRNAs from miRBase version 21 (Kozomara and Griffiths-Jones 2014) and quantified using the script quantifier.pl (a component of miRDeep2) using options –d and –t mmu. The defaults we used allow one mismatch and allow 2 nucleotides upstream and 5 nucleotides downstream of the mature sequence.

For each miRNA, we normalized the number of reads in each sample by the total number of miRNA-matching reads, then found all miRNAs with >1000 RPM (well-expressed) in at least one sample. We then combined those miRNAs that come from the same miRNA family, as defined by having the same composition at nucleotides 2-8. We used the raw read counts for those miRNA families when finding fold-change differences and differential expression using edgeR (Robinson *et al.* 2010). When using edgeR, we calculated normalization factors, estimated common and tagwise dispersion, and performed exact tests on each adult and neonatal pair for naïve, 5-dpi, and 7-dpi samples. The p-values are multiple test corrected using the Benjamini-Hochberg method.

Clustering was performed using the Euclidean method in the R package gplots. Principal component analysis was performed on $\log_{10}$(RPM) values for the miRNAs with >1000 RPM in at least one sample.

mRNA-Seq analysis. We trimmed nucleotides from the ends of sequencing reads if they had Phred quality scores <20. Reads that were at least 20 nucleotides long after trimming were aligned to the genome (mm9) using Tophat (Trapnell *et al.* 2009) with the option --no-novel-juncs. We used the mm9 GTF file provided by UCSC (available from the Tophat website). Differential expression of genes between samples was determined using CuffDiff (Trapnell *et al.* 2013) with a false discovery rate of 5%.

Clustering gene expression data. We clustered expressed genes that were significantly differentially expressed, and had at least a 2-fold difference in expression between adults and neonates in at least one sample (naïve, 5-dpi, 7-dpi, or 15-dpi). Those genes were grouped into five clusters using the partioning around medoids method (Reynolds *et al.* 2006) in R.

Enrichment statistics. Gene sets were downloaded from the Immunologic Signatures collection at the Molecular Signatures Database (MSDB). We found the number of genes from each dataset that belonged to a cluster. For each cluster, we found the number of genes that were found in both the cluster and the dataset (b), the total number of genes present in that cluster (n), the number of genes in the MSDB dataset (B), and the total number of genes that had been clustered (N). Enrichment was calculated as $\frac{b/n}{B/N}$. One-sided Fisher exact tests were used to measure significance.

3'-Seq. 3'-Seq was performed as described in (Lianoglou *et al.* 2013) (full protocol available at http://www.mskcc.org/sites/www.mskcc.org/files/node/25002/documents/3%27-seq%20protocol.pdf). Briefly, 1 ug of DNase-treated (Ambion) total RNA was incubated with a biotinylated polyT primer that contained a single RNA base (IDT) and Dynabeads M280 Steptavidin (Life Technologies). The RNA attached to the beads underwent first strand synthesis with SuperScriptIII (Life Technologies), then second strand synthesis with DNA Pol I (NEB) and RNaseH (NEB). The cDNA was nicked using RNase HII to introduce then translated with DNA Pol I (NEB) for 8 minutes at 8°C. After stopping the reaction with EDTA at 50 mM, the ends were cleaned up with T7 exonuclease (NEB), mung bean exonuclease (NEB), and Klenow enzyme (NEB) supplemented with dNTPs. Adapters were ligated with T4 DNA ligase (NEB), then amplified with Phusion (Fermentas). After the libraries were purified by PAGE, they were sequenced on the Hi-Seq platform with 100 bp reads.

3'-Seq analysis. To ensure that we were examining reads that captured the ends of 3'UTRs, we required that 3'-Seq reads contain the 3' adapter sequence adjacent to a stretch of A's. We then trimmed the A's and the adapter sequence from the 3' end of the read, then trimmed low quality nucleotides (Phred <20) from the 5' and 3' end of the read. Trimmed reads that were at least 20 nucleotides long, and were not derived from rRNA (removed using local alignment Bowtie2)Langmead *et al.* 2009; Langmead and Salzberg 2012), were then mapped to the mouse genome (mm9) using Tophat. The 3' end of uniquely matching reads were mapped and counted using the Genomecov tool from Bedtools (Quinlan and Hall 2010). We kept reads that mapped either in an annotated mouse 3'UTR (RefSeq, mm9) or within 1500 nt downstream, and we only considered the longest annotated 3'UTR isoform for genes that are reported to have multiple isoforms. We then determined which reads were within 50 nucleotides of a putative polyadenylation sequence (PAS, AATAAA or ATTAAA), and used those in further analyses. For each gene, an isoform was considered if it contained at least 20% of the reads for that gene. For genes that were targets of miR-29a-3p or miR-130b-3p and that did not end at the annotated position, we used TargetScan Mouse release 6.2 (Friedman

et al. 2009; Garcia *et al.* 2011)to determine if any miRNA target sites were lost in the shorter isoforms, using information from the files Conserved site context+ scores.txt and Nonconserved site context+ scores.txt.

Cloning. We used nested PCR to amplify fragments of 3'UTRs from genomic mouse DNA (Promega). The PCR primers were flanked with a SacI site on the forward oligo and a NotI site on the reverse oligo. We digested the PCR products and pmirGlo (Promega) with SacI-HF and NotI-HF (NEB), then ligated them with T4 DNA Ligase (NEB). We used site-directed mutagenesis (Agilent) to mutate the miRNA target sites at two positions. Our oligo sequences are:

Eomes	Outer PCR, forward	AACTAAACTGAAGCAGACCTAGCA
Eomes	Outer PCR, reverse	TGACCAAGGAAAGAGGATTAAGCA
Eomes	Inner PCR, forward	ATATATGAGCTCATGGGAAACGAGAAATGTTCAGAA
Eomes	Inner PCR, reverse	ATATATGCGGCCGCCGAAGTGGACAGAATATCTCCAAG
Tbx21	Outer PCR, forward	AGGTGCCCACTAACTTAGAAAACA
Tbx21	Outer PCR, reverse	ACCAGGTCCATGTTTATTTCCAGA
Tbx21	Inner PCR, forward	ATATATGAGCTCGGATTCTGGGGTTTACTTCTTGTT
Tbx21	Inner PCR, reverse	ATATATGCGGCCGCCCAGAAAGTGATGCAAAACAGAAG
Bak1	Outer PCR, forward	CCTGGCTGGACTAAACCTCTCT
Bak1	Outer PCR, reverse	TGAAGGTGGGGTTCAAGTAATCAT
Bak1	Inner PCR, forward	ATATATGAGCTCCTGGACTAAACCTCTCTCCCTAC
Bak1	Inner PCR, reverse	ATATATGCGGCCGCATGGATGGATTGGGGTAGGAGATA
Cd69	Outer PCR, forward	CACCACAGGAAAGTTGTGTAACTG
Cd69	Outer PCR, reverse	AACAGGTTATGTGACAAGACTGGA
Cd69	Inner PCR, forward	ATATATGAGCTCGACTGCACAAACCAACTTTACATC
Cd69	Inner PCR, reverse	ATATATGCGGCCGCCCTTGAAATACGCTACAGAGGTTT
Irf1	Outer PCR, forward	CTTGACACATGGCAAAGCATAGTC
Irf1	Outer PCR, reverse	CATGACCAAACACCATTTAGCAGT
Irf1	Inner PCR, forward	ATATATGAGCTCTCTGAGTTTTCTTGTGAGGTGAAG
Irf1	Inner PCR, reverse	ATATATGCGGCCGCATAGATAGTCAAGAGTCACGCCAA
Il6st	Outer PCR, forward	TAAAGACGAGTGGCTTCAGATGAG
Il6st	Outer PCR, reverse	CTGTAGGAGGACTTCTGTCATTGT
Il6st	Inner PCR, forward	ATATATGAGCTCCTTCAGATGAGAAACAGTCCTCAC

Il6st	Inner PCR, reverse	ATATATGCGGCCGCATAATAAGCAGTTTCTTGGGAGGC
Eomes upstream	Mutagenize miR-29 site, F	GCTATGAAGAACGAGTGCCCGGTACCATTAAATGAATTTCAAAG
Eomes downstream	Mutagenize miR-29 site, F	GGTATCAGATAAAAATAATGTAAATTTGGTACCTTGGCGTTGTAAAGAATTTGC
Tbx21	Mutagenize miR-29 site, F	CAGTCACGAACCTGGTACCGCTTCTGACCCC
Tbx21	Mutagenize miR-29 site, R	GGGGTCAGAAGCGGTACCAGGTTCGTGACTG
Bak1	Mutagenize miR-29 site, F	CCCCAACATTGCATGGTACCACTGAACCCCATCC
Bak1	Mutagenize miR-29 site, R	GGATGGGGTTCAGTGGTACCATGCAATGTTGGGG
Cd69	Mutagenize miR-130 site, F	CCAGTGCCTTTACGCATTAGCGCTATTTGGAGGGGTTTC
Cd69	Mutagenize miR-130 site, R	GAAACCCCTCCAAATAGCGCTAATGCGTAAAGGCACTGG
Irf1	Mutagenize miR-130 site, F	CTCTGTACTAGGAGACAATAGCGCTAAATGAGTCCTATTCCC
Irf1	Mutagenize miR-130 site, R	GGGAATAGGACTCATTTAGCGCTATTGTCTCCTAGTACAGAG
Il6st	Mutagenize miR-130 site, F	GTGCTCTTTCAGAATGTTAGCGCTGCCGAAAACAAAGTGTGTC
Il6st	Mutagenize miR-130 site, R	GACACACTTTGTTTTCGGCAGCGCTAACATTCTGAAAGAGCAC

Cell culture. HEK293 cells were used because they express negligible amounts of miR-29 and no detectable miR-130 (Mayr and Bartel 2009). They were maintained in DMEM (Gibco) supplemented with 10% FBS and penicillin/streptomycin at 37°C with 5% CO_2. At 24-hours before transfection, we plated cells at 50,000 cells/mL in 24-well plates. We transfected 10 ng of the experimental plasmid and 25 nmol of miRNA mimic (IDT) using Lipofectamine 2000 (Life Technologies). We harvested the cells 24 hours later and stored them at -80°C. Luciferase amounts for Firefly and *Renilla* were measured using the Dual-Luciferase Reporter Assay system (Promega) with a dual-injection luminometer (Turner Biosystems). Firefly luciferase luciferase levels were normalized to *Renilla*. The miRNA mimic sequences are:

miR-29 sense strand	UAGCACCAUCUGAAAUCGGUUA
miR-29 anti-sense strand	ACCGAUUUCAGAUGGUGUUAAU
miR-130 sense strand	CAGUGCAAUGUUAAAAGGGCAU
miR-130 anti-sense strand	GCCCUUUUAACAUUGCACAGAU

Files S2-S7

Available for download at www.genetics.org/lookup/suppl/doi:10.1534/genetics.115.179176/-/DC1

File S2 Expression values (reads per million) for miRNAs that are well-expressed in at least one sample.

File S3 Fold-change expression changes between adults, neonates, and newborns for miRNA families.

File S4 Gene expression of miRNA targets.

File S5 Positions and expression of 3'UTR isoforms.

File S6 Expression and differential expression information for expressed genes.

File S7 Genes present in clusters.

Literature Cited

Friedländer M. R., Mackowiak S. D., Li N., Chen W., Rajewsky N., 2012 miRDeep2 accurately identifies known and hundreds of novel microRNA genes in seven animal clades. Nucleic Acids Res. **40**: 37–52.

Friedman R. C., Farh K. K.-H., Burge C. B., Bartel D. P., 2009 Most mammalian mRNAs are conserved targets of microRNAs. Genome Res. **19**: 92–105.

Garcia D. M., Baek D., Shin C., Bell G. W., Grimson A., Bartel D. P., 2011 Weak seed-pairing stability and high target-site abundance decrease the proficiency of lsy-6 and other microRNAs. Nat. Struct. Mol. Biol. **18**: 1139–1146.

Kozomara A., Griffiths-Jones S., 2014 miRBase: annotating high confidence microRNAs using deep sequencing data. Nucleic Acids Res. **42**: D68–D73.

Langmead B., Trapnell C., Pop M., Salzberg S. L., 2009 Ultrafast and memory-efficient alignment of short DNA sequences to the human genome. Genome Biol. **10**: R25.

Langmead B., Salzberg S. L., 2012 Fast gapped-read alignment with Bowtie 2. Nat. Methods **9**: 357–359.

Lewis B. P., Burge C. B., Bartel D. P., 2005 Conserved Seed Pairing, Often Flanked by Adenosines, Indicates that Thousands of Human Genes are MicroRNA Targets. Cell **120**: 15–20.

Lianoglou S., Garg V., Yang J. L., Leslie C. S., Mayr C., 2013 Ubiquitously transcribed genes use alternative polyadenylation to achieve tissue-specific expression. Genes Dev. **27**: 2380–2396.

Mayr C., Bartel D. P., 2009 Widespread shortening of 3'UTRs by alternative cleavage and polyadenylation activates oncogenes in cancer cells. Cell **138**: 673–684.

Quinlan A. R., Hall I. M., 2010 BEDTools: a flexible suite of utilities for comparing genomic features. Bioinformatics **26**: 841–842.

Reynolds A. P., Richards G., Iglesia B. de la, Rayward-Smith V. J., 2006 Clustering Rules: A Comparison of Partitioning and Hierarchical Clustering Algorithms. J. Math. Model. Algorithms **5**: 475–504.

Robinson M. D., McCarthy D. J., Smyth G. K., 2010 edgeR: a Bioconductor package for differential expression analysis of digital gene expression data. Bioinforma. Oxf. Engl. **26**: 139–140.

Trapnell C., Pachter L., Salzberg S. L., 2009 TopHat: discovering splice junctions with RNA-Seq. Bioinformatics **25**: 1105–1111.

Trapnell C., Hendrickson D. G., Sauvageau M., Goff L., Rinn J. L., Pachter L., 2013 Differential analysis of gene regulation at transcript resolution with RNA-seq. Nat. Biotechnol. **31**: 46–53.